NTP Satellite Symposium - "Pathology Potpourri"

Toxicologic Pathology, 39: 240-266, 2011

ISSN: 0192-6233 print / 1533-1601 online
DOI: 10.1177/0192623310391680

Proceedings of the 2010 National Toxicology Program Satellite Symposium

E. Terence Adams[1], Scott Auerbach[2], Pamela E. Blackshear[3], Alys Bradley[4], Margarita M. Gruebbel[1], Peter B. Little[5], David Malarkey[2], Robert Maronpot[6], Jennifer S. McKay[7], Rodney A. Miller[1], Rebecca R. Moore[1], James P. Morrison[5], Abraham Nyska[8], Yuval Ramot[9], Deepa Rao[2,3], Andrew Suttie[10], Monique Y. Wells[11], Gabrielle A. Willson[1], and Susan A. Elmore (Chair)[2]

[1]*Experimental Pathology Laboratories, Inc., Research Triangle Park, NC, USA*
[2]*National Toxicology Program, National Institute of Environmental Health Sciences, National Institutes of Health, Research Triangle Park, NC, USA*
[3]*Integrated Laboratory Systems, Inc., Research Triangle Park, NC, USA*
[4]*Charles River Laboratories, Tranent, Edinburgh, United Kingdom*
[5]*Charles River Laboratories, Pathology Associates, Durham, NC, USA*
[6]*Maronpot Consulting, LLC, Raleigh, NC, USA*
[7]*AstraZeneca, Macclesfield, United Kingdom*
[8]*Consultant in Toxicological Pathology, Sackler School of Medicine, Tel Aviv University, Israel*
[9]*Department of Dermatology, Hadassah—Hebrew University Medical Center, Jerusalem, Israel*
[10]*Covance Laboratories, Inc., Vienna, VA, USA*
[11]*Toxicology/Pathology Services, Inc., Paris, France*

Abstract

The 2010 annual National Toxicology Program (NTP) Satellite Symposium, entitled "Pathology Potpourri," was held in Chicago, Illinois, in advance of the scientific symposium sponsored jointly by the Society of Toxicologic Pathology (STP) and the International Federation of Societies of Toxicologic Pathologists (IFSTP). The goal of the annual NTP Symposium is to present current diagnostic pathology or nomenclature issues to the toxicologic pathology community. This article presents summaries of the speakers' presentations, including diagnostic or nomenclature issues that were presented, along with select images that were used for voting or discussion. Some topics covered during the symposium included a comparison of rat and mouse hepatocholangiocarcinoma, a comparison of cholangiofibrosis and cholangiocarcinoma in rats, a mixed pancreatic neoplasm with acinar and islet cell components, an unusual preputial gland tumor, renal hyaline glomerulopathy in rats and mice, eosinophilic substance in the nasal septum of mice, INHAND nomenclature for proliferative and nonproliferative lesions of the CNS/PNS, retinal gliosis in a rat, fibroadnexal hamartoma in rats, intramural plaque in a mouse, a treatment-related chloracne-like lesion in mice, and an overview of mouse ovarian tumors.

Keywords: NTP Satellite Symposium; INHAND nomenclature; hepatocholangiocarcinoma; acinar-islet cell; preputial gland; hyaline glomerulopathy; eosinophilic substance; ependymoma; axonal degeneration; retinal gliosis; fibroadnexal hamartoma; intramural plaque; chloracne; ovary; cholangiocarcinoma.

Introduction

The National Toxicology Program (NTP) Satellite Symposium is a one-day meeting that is traditionally held in conjunction with the annual scientific symposium of the Society of Toxicologic Pathology (STP) (Bach et al. 2010). Continuing education on the interpretation of pathology slides

Address correspondence to: Susan A. Elmore, National Toxicology Program, Cellular and Molecular Pathology Branch, National Institute of Environmental Health Sciences, National Institutes of Health, Research Triangle Park, NC 27709, USA; e-mail: elmore@niehs.nih.gov.

This research was supported (in part) by the Intramural Research Program of the National Institute of Environmental Health Sciences (NIEHS), of the National Institutes of Health (NIH). This article may be the work product of an employee or group of employees of the NIEHS. However, the statements, opinions, or conclusions contained herein do not necessarily represent the statements, opinions, or conclusions of NIEHS, NIH, or the United States government.

Abbreviations: BSTP, British Society of Toxicological Pathologists; CNS, central nervous system; DLC, dioxin-like compound; EM, electron microscopy; F344/N, Fischer 344/N; FCH, folliculosebaceous cystic hamartoma; GFAP, glial fibrillary acidic protein; GLAST, glutamate aspartate transporter; HCCC, hepatocholangiocarcinoma; HCD, historical control data; H&E, hematoxylin and eosin; IFSTP, International Federation of Societies of Toxicologic Pathologists; IHC, immunohistochemistry/immunohistochemical; INHAND, International Harmonization of Nomenclature and Diagnostic Criteria for Lesions in Rats and Mice; MnSOD, manganese superoxide dismutase; NIEHS, U.S. National Institute of Environmental Health Sciences; NTP, U.S. National Toxicology Program; OWG, organ working group; PAS, periodic acid-Schiff; PNS, peripheral nervous system; PTAH, phosphotungstic acid-hematoxylin; SCC, squamous cell carcinoma; STP, Society of Toxicologic Pathology; TCAB, 3,3',4,4'-tetrachloroazobenzene.

has been the primary goal of the NTP Symposium. To achieve this goal, multiple presentations show and discuss lesions that are rare and interesting, present a diagnostic challenge, are controversial, and/or have nomenclature dilemmas. Audience participation is encouraged through anonymous voting with wireless keypads and real-time tabulation software. The voting results are immediately displayed on the screen as bar graphs with voting percentages, which allows for lively and productive discussion with audience members immediately after the voting.

The theme of the NTP Symposium in previous years, spanning 2000 to 2009, has been kept flexible to allow for current issues to be presented. In some years the entire session focuses on a single theme; past topics included tumor pathology, pathology of the urinary system, pathology of the immune system, hepatic pathology, an exercise in peer review: the pathology working group, techniques in toxicologic pathology, and establishing an NTP database for non-neoplastic lesions of kidney and urinary bladder. For two of these years, the theme has been ''pathology potpourri,'' in which a number of lesions and issues are dealt with briefly. For 2010, the ''pathology potpourri'' theme was used again, allowing the presentation of unusual lesions in the liver, pancreas, preputial gland, kidney, nasal septum, retina, skin, lung, ovary, and vascular system. Also included were example definitions and discussion of proposed INHAND **(In**ternational **Ha**rmonization of **N**omenclature and **D**iagnostic Criteria for Lesions in Rats and Mice) nomenclature for proliferative and nonproliferative entities of the central (CNS) and peripheral (PNS) nervous system and cardiovascular system. This input from the toxicologic pathology community is of value as the Organ Working Groups are preparing their draft nomenclature documents. This article provides synopses of all presentations including the diagnostic or nomenclature issues, a selection of images presented for voting and discussion, voting choices, voting results, and major discussion points.

Rat and Mouse: Are They Really That Different?

A presentation on rat hepatocholangiocarcinoma (HCCC) by Dr. Rodney A. Miller (Experimental Pathology Laboratories, Inc., Research Triangle Park, NC, USA) was based on the collaborative work of Drs. Rebecca Moore, Gabrielle Willson, and David Malarkey. After presentation of several images of a primary liver tumor and metastatic lesions in the lung and heart from a male Fischer 344/N (F344/N) rat, a vote was taken in which the participants were given the following choices: (1) hepatocellular carcinoma, (2) atriocaval mesothelioma, (3) hepatoblastoma, (4) HCCC, and (5) hepatocholangioma. HCCC was the correct response and received 73% of the votes. The other votes recorded were hepatocellular carcinoma (17%), atriocaval mesothelioma (4%), hepatoblastoma (4%), and hepatocholangioma (2%).

After the vote, Dr. Miller gave a presentation on rat HCCC in the NTP database of chronic carcinogenicity studies (305 two-year bioassays conducted from 1982 to 2008) and compared the morphology and behavior of HCCC in F344/N rats to those in B6C3F1 mice. HCCC is defined as a primary liver neoplasm containing a combination of neoplastic hepatocytes and neoplastic biliary epithelial cells, both exhibiting malignant characteristics (Figures 1A and 1B). The incidence of HCCC in treated F344/N rats was less than 1%, yielding a total of 73 HCCCs (29 male and 44 female rats) from six studies. HCCC occurred less commonly in males (40%) than in females (60%), and none were observed in control rats. There was one primary HCCC observed per affected animal. Metastases were evident in 5 of the 73 animals (6.9%). All 5 rats with metastatic lesions exhibited multiple foci of lung involvement; the only other site of metastasis was the heart, which was noted in only 1 animal. HCCCs were considered to be treatment related in two studies: methyleugenol (NTP 2000) and 1-amino-2,4-dibromoanthraquinone (NTP 1996). In both studies there was a concomitant treatment-related increase in hepatocellular adenomas and carcinomas in both sexes.

The malignant hepatocellular component in all HCCC cases exhibited a trabecular growth pattern, which was characterized by prominent cords of hepatocytes three or more cell layers thick. The malignant biliary component consisted of exuberant proliferating epithelial cells forming ducts that were markedly variable in size. Often there was intermixing of neoplastic hepatocytes and neoplastic biliary epithelium in the same cord (Figure 1C). Necrosis and cystic degeneration were common within the primary neoplasm. Only one rat had metastatic lesions, in the heart and lung, composed of both the hepatocellular and biliary components (Figures 1D and 1E). Metastatic lesions in the remaining four rats were restricted to the lung and exhibited only hepatocellular features.

In contrast to the F344/N rat, HCCC in B6C3F1 mice is an aggressive neoplasm that metastasizes readily to numerous organs, at a rate of 84% (Bach et al. 2010). While HCCC in mice is reportedly induced by chemicals such as benzidine dihydrochloride and N-2-acetylaminofluorene (Frith, Ward, and Turusov 1994), treatment-related HCCCs in mice were not observed in the NTP data set of 2-year carcinogenicity studies. HCCC was more commonly observed in male mice than female mice and was seen in control groups. In about 16% of the mice with HCCC, foci of undifferentiated cells, often with a sarcomatous appearance, occurred within the primary tumor. This morphologic feature was not observed in the rat. In both mice and rats, identification of HCCC may prove a diagnostic challenge, because lack of familiarity with rare tumors renders misdiagnosis more likely. The presence of both neoplastic hepatocellular and neoplastic biliary components in liver tumors should prompt the diagnosis of HCCC.

In summary, HCCC is a rare tumor in rats and mice, the incidence and behavior of which differs substantially between the species. HCCC is seen in up to 10% of control mice, but HCCC has not been diagnosed in control rats. Treatment-related HCCCs have been observed in rats in two NTP studies but have not been induced in mice by any treatment in any NTP study. HCCC in the F344/N rat metastasizes at a low rate (7%) only to the lung and heart, while HCCC in

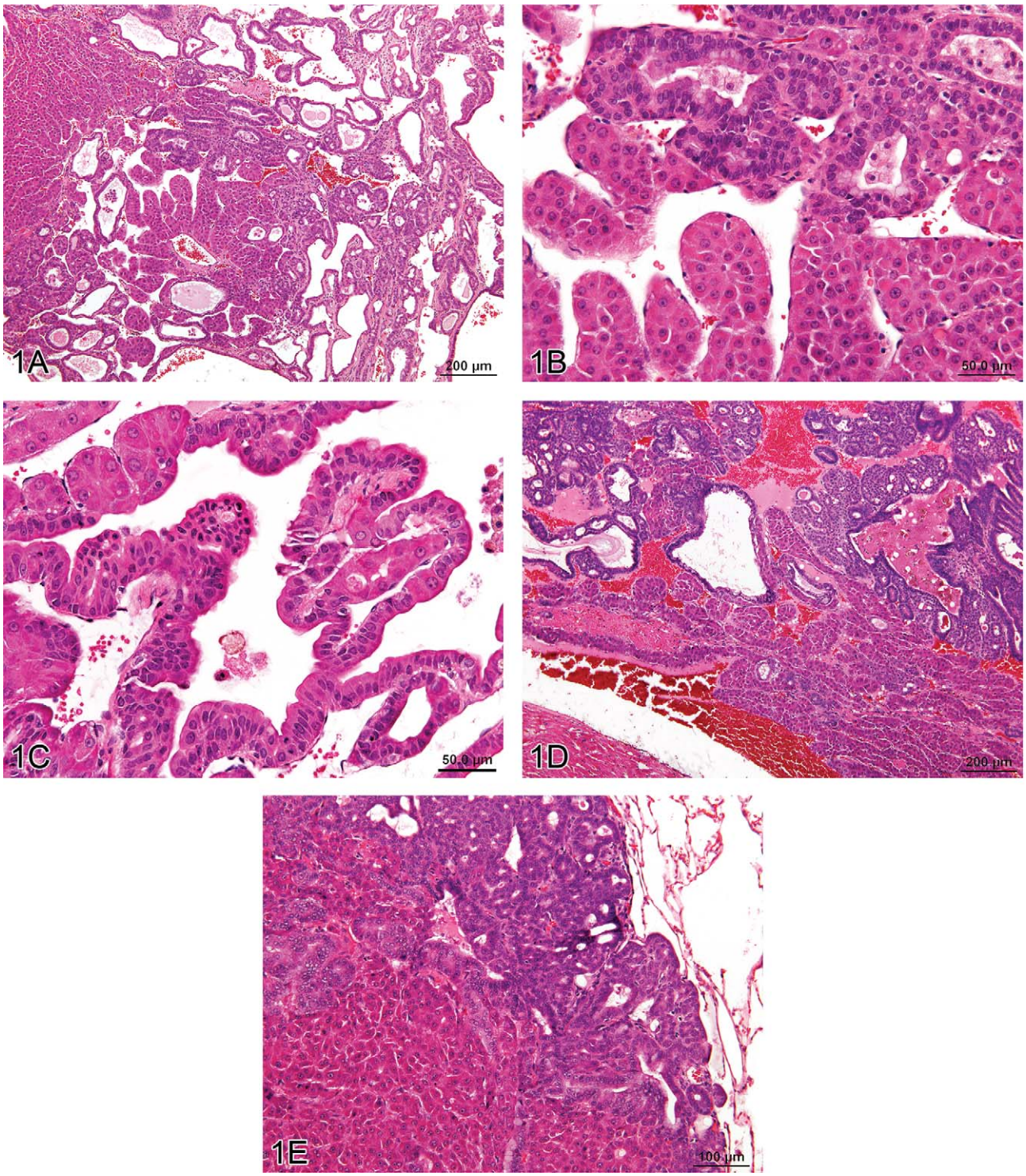

FIGURE 1.—Hepatocholangiocarcinoma (HCCC), a primary hepatic tumor containing both neoplastic hepatocellular and neoplastic biliary epithelial elements. (A) Typical trabecular morphology of hepatocellular carcinoma in conjunction with exuberant neoplastic biliary epithelial proliferation. (B) Neoplastic trabeculae are at least 3 cell layers thick and (C) blend proliferating hepatocytes and biliary epithelial cells in the same cords. Metastases of HCCC in the heart (D) and lung (E) contain both proliferating hepatocytes and biliary epithelial cells. H&E.

B6C3F1 mice aggressively spreads to many organs in most animals (84%). Some primary liver tumors and metastatic lesions in mice had areas of undifferentiated cells (sarcoma-like), which were not observed in rat HCCC. Clearly, morphologically similar entities in mice and rats may possess widely divergent biological properties, thereby confirming that mice are not just different-sized versions of a single model species.

Cholangiofibrosis versus Cholangiocarcinoma

After illustrating unequivocal examples of intrahepatic cholangioma and cholangiocarcinoma, Dr. Robert Maronpot (Maronpot Consulting, LLC, Raleigh, NC, USA) introduced cholangiofibrosis, a controversial intrahepatic cholangial lesion defined by proliferative, metaplastic, and inflammatory components. Several xenobiotics have been shown to induce this hepatic change, which occurs exclusively in chemically treated rats (Bannasch and Zerban 1990; Deschl et al. 1997; Eustis et al. 1990; Kimbrough et al. 1973; Kimbrough and Linder 1974; Sirica 1992; Hailey et al. 2005). Cholangiofibrosis and a putatively related, seemingly malignant lesion are morphologically similar at high magnifications. Even within a single animal, this lesion is highly variable in the extent of liver involvement, ranging from affected subcapsular areas to irregular patches within hepatic lobes to total involvement of entire lobes (Figures 2A and 2B). With the exception of subcapsular lesions with extensive dilation of proliferative glandular structures (see Figure 2C), cholangiofibrosis tends to be contractile rather than expansive (especially when viewed at low magnification). Morphological features at high magnification include dilated glands lined by hyperbasophilic and metaplastic epithelium (intestinal metaplasia), which contain necrotic debris and/or mucus, an inflammatory cell infiltrate, and fibrosis (Figures 2D and 2E). In some instances, the cholangiofibrosis is disseminated throughout the liver (Figure 2D).

Dr. Maronpot indicated that distinguishing between benign and malignant forms of this cholangial lesion is arbitrary and traditionally has been based largely on lesion size or the extent of liver involvement rather than on any definitive morphological features. He pointed out that unequivocal evidence for metastasis of these lesions has not been seen, and was of the opinion that all these proliferative and metaplastic, intrahepatic cholangial lesions were variations of benign cholangiofibrosis and not malignancies. He indicated that if a diagnosis of cholangiocarcinoma was appropriate and/or preferred, it could be called ''cholangiocarcinoma, intestinal type'' as previously proposed (Greaves 2007).

Following presentation of lesions previously diagnosed and confirmed by peer review to be either cholangiofibrosis or cholangiocarcinoma, Dr. Maronpot presented four cases for audience voting. In all cases, the voting choices were cholangioma; cystic cholangioma; cholangiocarcinoma; cholangiofibrosis; cystic cholangiofibrosis; and cholangiocarcinoma, intestinal type. Case 1 from a treated female Sprague-Dawley rat was originally diagnosed as cholangiocarcinoma and had extensive involvement of hepatic parenchyma with active glandular formation at the lesion perimeter. The audience vote was split, with approximately half voting for cholangiofibrosis and 25% choosing cholangiocarcinoma, intestinal type. Case 2 was a lesion with extensive glandular proliferation involving greater than 90% of the hepatic parenchyma from a high-dose F344/N rat exposed to estragole for 90 days. Based on the extensive parenchymal involvement, this lesion was originally diagnosed as a cholangiocarcinoma. The audience voting favored a diagnosis of cholangiocarcinoma, intestinal type (34%), with only 26% voting for cholangiofibrosis. Case 3 was a lesion characterized by solid sheets of proliferating biliary cells with some dilated, metaplastic glands from a high-dose F344/N rat given furan for 90 days. The original diagnosis was cholangiofibrosis, but the solid cell sheets influenced 74% of the audience to select cholangiocarcinoma Case 4, from a treated, female, Sprague-Dawley rat, was a small lesion characterized by dilated, mucus-filled glands on the liver surface. This lesion was originally diagnosed as a cholangiofibrotic nodule; the majority of the audience (60%) voted for cholangiofibrosis, with most favoring a ''cystic'' qualifier for the diagnosis.

In conclusion, audience opinion did not favor the use of ''cholangiocarcinoma, intestinal type.'' Instead, the general feeling was that large lesions with morphological features common to cholangiofibrosis that might warrant a diagnosis of malignancy, even in the absence of metastasis, should be diagnosed as cholangiocarcinoma, and the morphological features should be described in detail in the pathology narrative. This would avoid any potential confusion that introduction of a different category of cholangiocarcinoma might cause. An additional concern was that the term cholangiofibrosis did not adequately address the biliary hyperplastic feature of the lesion, although an alternative diagnosis was not presented or discussed.

Is It This, or Is It That?

Another vignette, given by Dr. Margarita Gruebbel (Experimental Pathology Laboratories, Inc., Research Triangle Park, NC, USA), presented two rare neoplasms that had challenging and/or unusual morphology.

The first case was a pancreatic lesion in a control male F344/N rat necropsied on day 731 at the end of a NTP 2-year carcinogenicity bioassay. The small, encapsulated, slightly compressive tumor consisted of approximately equal proportions of islet cells and acinar cells intermingled in a mosaic-like pattern (Figures 3A and 3B). In some areas the neoplastic islet cells were arranged in small, tightly packed nests, but in others they formed invasive sheets (Figure 3C) (Riley et al. 1990). Neoplastic islet cells had indistinct membranes; abundant, pale eosinophlic cytoplasm; variably sized but usually large, oval to round nuclei with finely stippled chromatin and central nucleoli; and occasional mitotic figures (Figure 3D). Clusters of acinar cells usually formed acini with narrow lumens that were bounded by basal lamina, which separated them from the surrounding islet cells. Compared to normal exocrine cells, the neoplastic acinar cells were generally large; had more abundant pale blue cytoplasm but fewer pale pink zymogen granules (Figures 3E and 3F); and possessed large, oval to round, vesicular nuclei with marginated chromatin and prominent, sometimes multiple nucleoli (Figure 3F). Mitotic figures were occasionally present (Figure 3E). Scattered among the acinar and islet elements were occasional ductules lined by

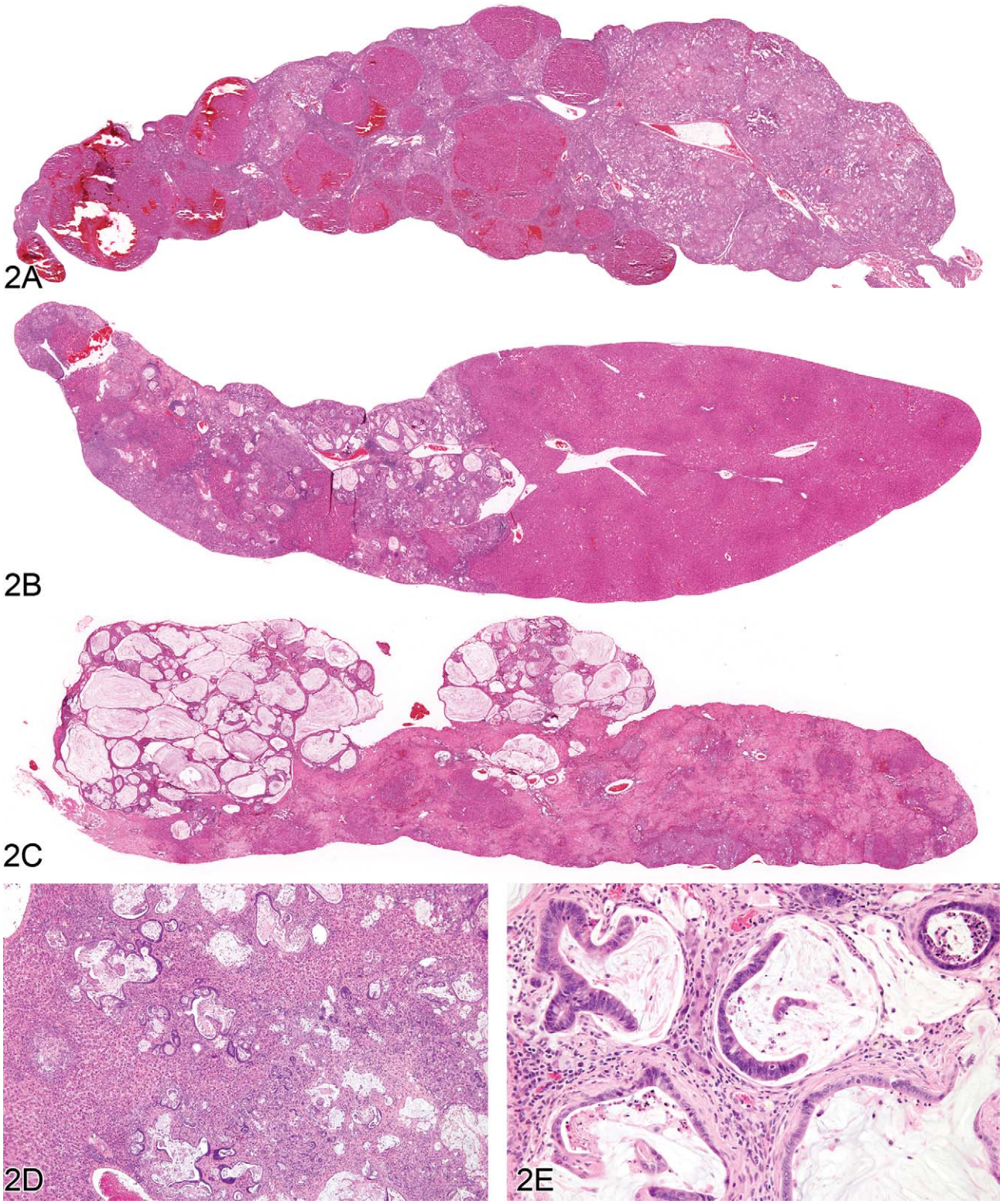

FIGURE 2.—Cholangiofibrosis in the rat. (A) A low-magnification image of a liver lobe from a F344/N rat treated with a high dose of furan for several months. A large portion of the lobe has been replaced by cholangiofibrosis with focal areas of regenerative hepatocellular hyperplasia. The overall contour of the lobe has not been appreciably expanded. (B) A different lobe from the same rat as in (A) with a localized contracted area of cholangiofibrosis. The remainder of the lobe is relatively normal. (C) Low-magnification image of a liver lobe from a F344/N rat treated with a high dose of furan for several months. Two protruding nodules of cholangiofibrosis on the surface of the liver consist of markedly dilated, mucus-filled glands. The remainder of the lobe is occupied by resolving sclerotic remnants of cholangiofibrosis. (D) Cholangiofibrosis diffusely distributed in the liver of a Sprague-Dawley rat treated with a high dose of a dioxin-related xenobiotic. Both small and mucus-filled, dilated biliary glands are present. (E) High magnification of 11D showing mucus-filled dilated glands with partial loss of glandular epithelium surrounded by inflammatory cell infiltrates and fibrosis. H&E.

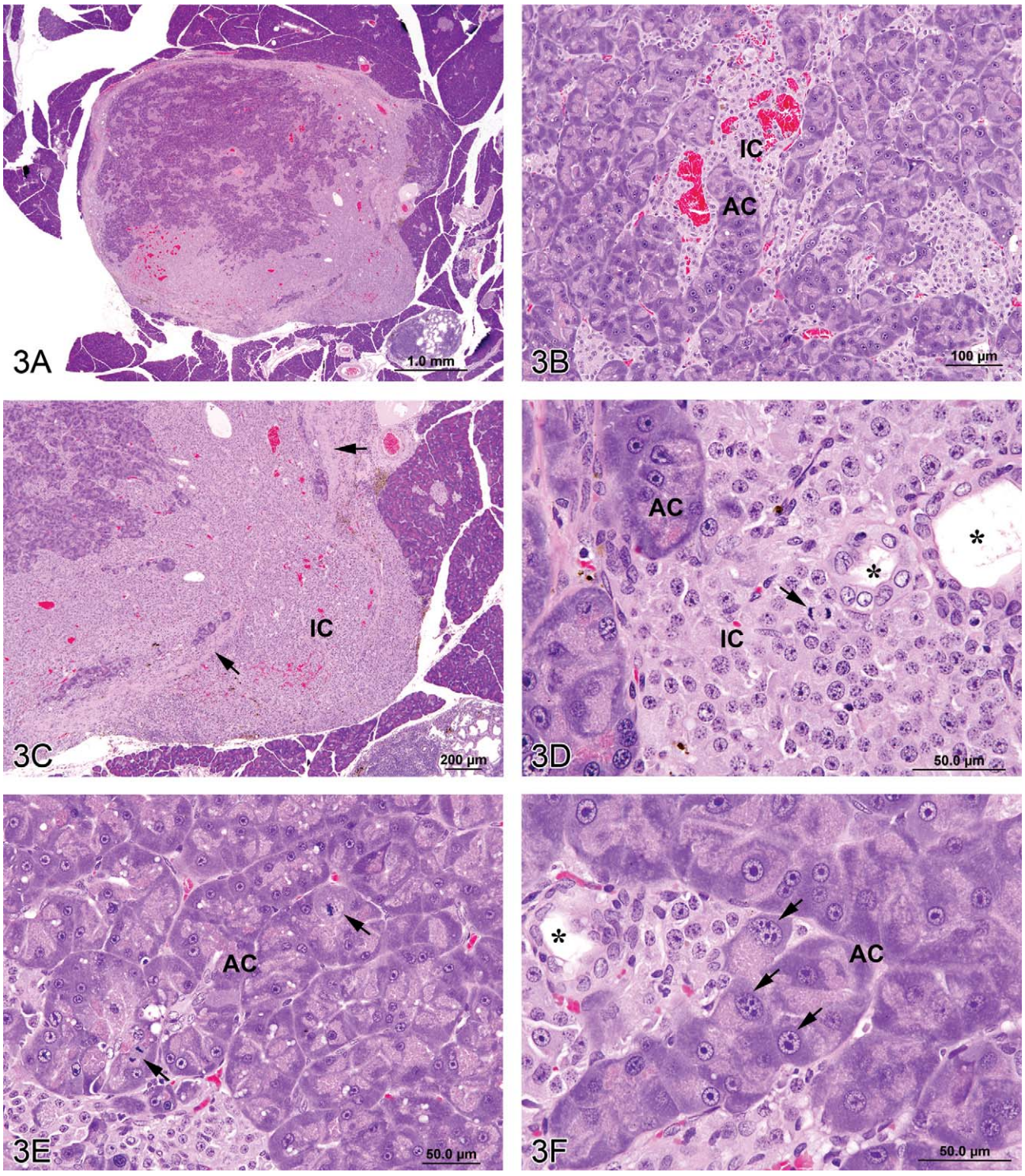

FIGURE 3.—Mixed tumors in the rat. (A) Pancreatic malignant mixed tumor from a male F344/N rat from a 2-year bioassay. (B) Higher magnification of the neoplasm in (A) showing intermingled but distinct acinar cell (AC) and islet cell (IC) components. (C) Extension of neoplastic IC across the fibrous capsule (arrows). (D) Neoplastic IC are pleomorphic and may have mitotic figures (arrow). Ductules (*) are lined by epithelial cells with abundant pale pink cytoplasm and large vesicular nuclei. (E) Pleomorphic neoplastic AC have abundant cytoplasm with decreased zymogen granules and sometimes mitotic figures (arrows). (F) Neoplastic AC are also characterized by large, vesicular nuclei with prominent, often multiple nucleoli (arrows). Ductules (*) are lined by epithelial cells with abundant pale pink cytoplasm and large vesicular nuclei.

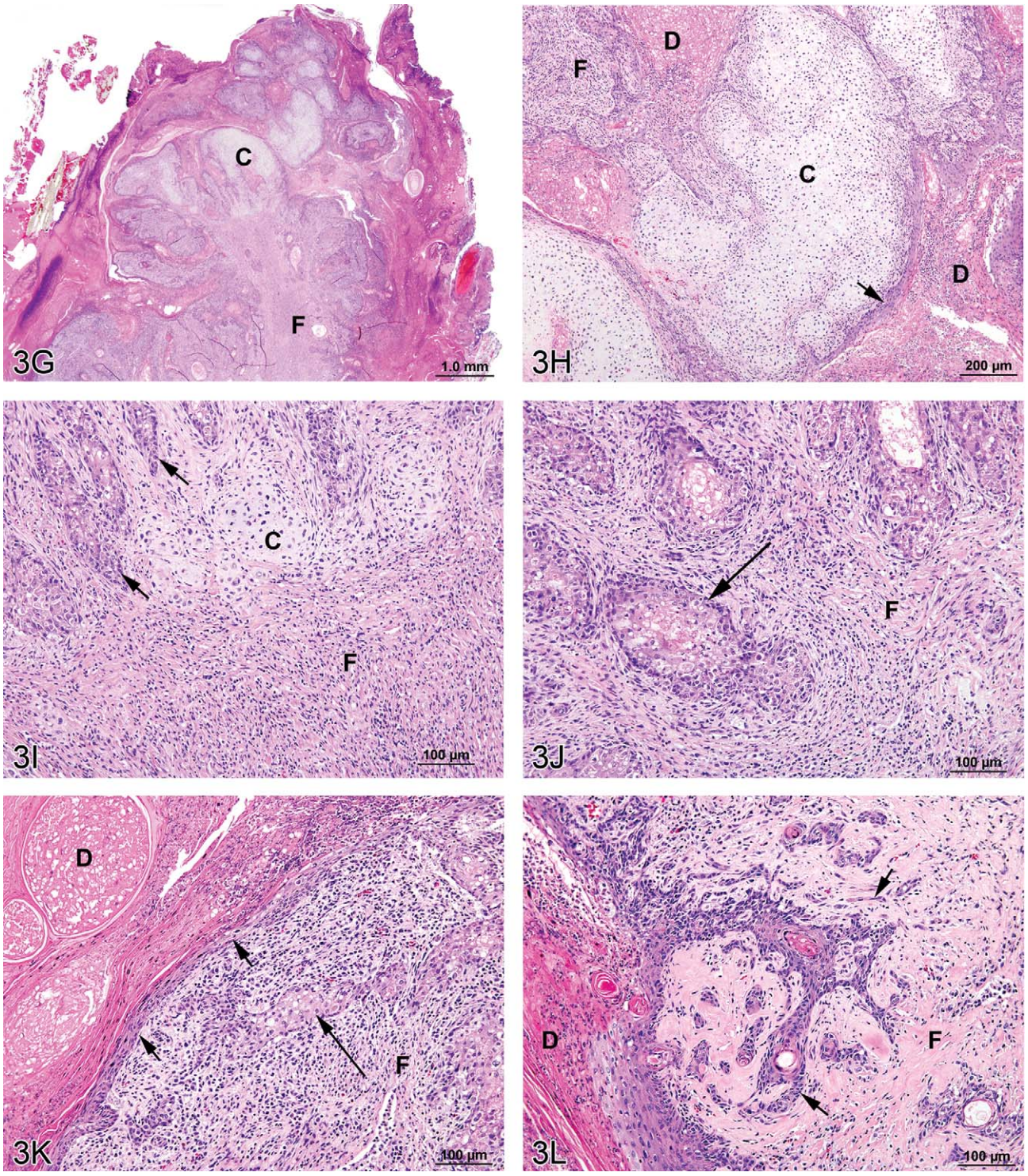

FIGURE 3.—**(continued)** (G) Preputial gland from a male F344/N rat from a 2-year bioassay. Extensive areas of cartilaginous (C) and fibrous (F) tissues compress and replace the normal glandular architecture. (H) Higher magnification of the mass exhibits cartilage (C) and fibrous connective tissue (F). Dilated ducts (D) are filled with necrotic debris, inflammatory cells, and keratin and lined by poorly differentiated epithelial cells (arrow). (I) Areas of cartilage (C) and fibrous connective tissue (F) in which are scattered acinar-like structures (arrows). Diffuse inflammatory cell infiltrates are present in the fibrous tissue (F). (J) Fibrous connective tissue (F) contains diffuse inflammatory cell infiltrates and surrounds poorly differentiated acinar-like structures (arrow). (K) Fibrous connective tissue (F) contains diffuse inflammatory cell infiltrates and surrounds poorly differentiated acinar-like structures (long arrow). The adjacent dilated duct (D) is distended by necrotic debris, keratin, and inflammatory cells and is lined by poorly differentiated squamous epithelium (short arrows). (L) The poorly differentiated squamous epithelium lining a dilated duct (D) exhibits extension of branching cords and "dropping off" of cell clusters and individual neoplastic cells (arrows) into the underlying fibrous connective tissue (F). H&E.

plump epithelial cells with pale pink cytoplasm and large, vesicular nuclei (Figures 3D and 3F).

The voting choices for this first lesion were (1) islet cell tumor, benign; (2) islet cell tumor, malignant; (3) mixed tumor, benign; (4) mixed tumor, malignant; (5) mixed acinar-islet cell tumor, malignant; and (6) acinar-islet cell carcinoma. The top choice was malignant mixed acinar-islet cell tumor (44%), with fewer votes for malignant islet cell tumor (16%), benign mixed tumor (14%), acinar-islet cell carcinoma (12%), malignant mixed tumor (11%), and benign islet cell tumor (3%). This case—which has undergone the NTP peer-review process—is recorded in the NTP database (1982–2010) as a pancreatic malignant mixed tumor. Thus, although the preferred diagnostic terms differed, there was general concurrence for a term denoting a malignant neoplasm with proliferative acinar and islet cell populations (81% of the votes).

During subsequent discussion, the possibility was raised that the intra-tumor acinar cells were non-neoplastic, and simply entrapped within an islet-cell tumor. However, in this case, the morphology of the acinar cells in the neoplasm was quite distinct from that of normal acinar cells, and was characterized by multiple traits consistent with a proliferative process: variable arrangement (solid nests or indistinct acini); more abundant, pale basophilic cytoplasm with fewer zymogen granules; pleomorphic nuclei; prominent, often multiple nucleoli; and occasional mitotic figures. The possibility that this case represented a ''collision'' of two separate neoplasms was also raised. However, rather than being restricted to particular zones with little intermingling (as might be expected in a collision situation), the acinar and islet cell populations were intimately interdigitated throughout the mass. It was also noted that neither this case nor any of the other pancreatic malignant mixed tumors in the NTP database (1982–2010) exhibited invasion or distant metastasis.

Pancreatic mixed tumors in rats have been described as having ''uniformly dispersed islet and acinar cells,'' both of which exhibit ''some degree of cytologic alteration'' (Eustis, Boorman, and Hyashi 1990). In rodents, these neoplasms have been referred to as pancreatic ''mixed acinar-islet cell'' neoplasms (Eustis, Boorman, and Hyashi 1990); ''mixed acinar-islet cell tumors'' (Riley et al. 1990); and ''acinar-islet cell'' neoplasms (Mohr 1994). They are rare, with only 46 cases in F344/N rats listed in the 1982 to 2010 NTP database.

The NTP cases occurred sporadically in control and treated rats, and all were considered incidental. Of these cases, 42 (91%) were adenomas and 4 (9%) were carcinomas. The great majority occurred in males (44 [96%]), with only 2 (both adenomas) in females. Corresponding mixed pancreatic neoplasms in humans are composed of morphologically and immunohistochemically (IHC) distinct acinar, islet, and/or ductular cell types (Klimstra, Rosai, and Heffess 1994; Marrache et al. 2005; Newman et al. 2009), while others are composed wholly or predominantly of a single ''amphicrine'' cell type exhibiting concurrent morphologic and IHC markers of at least two of these cell types (Klimstra, Rosai, and Heffess 1994; Terada et al. 1999). Proposed pathogeneses of these ''mixed'' pancreatic neoplasms in humans include bilinear or trilinear development from a putative multipotent stem cell (Klimstra, Rosai, and Heffess 1994; Newman et al. 2009), transdifferentiation of one neoplastic cell type into another type (Terada et al. 1999), or modulation of acinar cell proliferation via peptides secreted by neoplastic islet cells (Marrache et al. 2005). Whether any of these proposed mechanisms are also pertinent to the development of the pancreatic mixed acinar-islet cell tumors in rats remains undetermined.

Dr. Gruebbel's second case was an incidental preputial gland neoplasm from a mid-dose male F344/N rat from a NTP 2-year carcinogenicity bioassay. This animal was found dead on day 722 due to mononuclear cell leukemia. At necropsy, the left preputial gland was grossly dark and enlarged. Microscopically, the normal gland architecture was compressed and partly replaced by proliferative mesenchymal tissue (Figure 3G) consisting of coalescing, hyaline-like cartilage nodules alternating with sheets and interlacing bands of fibrous connective tissue (Figures 3H, 3I, 3J). Lateral duct branches intercalated between the cartilaginous/fibrous masses were lined by poorly differentiated squamous epithelial cells (Figures 3K, 3L) arranged in disorderly layers. Downward extension of branching cords and ''dropping off'' of epithelial cell nests and individual cells was evident in the underlying fibrous tissue (Figure 3L). Occasional solid nests or gland-like structures composed of crowded, poorly differentiated acinar cells (Figures 3I, 3J, and 3K). The fibrous and epithelial areas exhibited focal necrosis and variable but often abundant mixed infiltrates of inflammatory cells (Figures 3I, 3J, 3K). The central duct and its remaining larger lateral branches were focally ulcerated and distended by inspissated secretory material, sloughed keratin, inflammatory cells, and necrotic debris (Figures 3H, 3K, 3L).

The voting choices were (1) chondrosarcoma; (2) chondrofibrosarcoma; (3) carcinoma (with cartilaginous metaplasia); (4) carcinosarcoma; and (5) mixed tumor, malignant. The audience tally was carcinoma with cartilaginous metaplasia (28%), mixed tumor (26%), chondrofibrosarcoma (19%), chondrosarcoma (15%), and carcinosarcoma (13%). Thus, the voting indicated a wide range of opinion regarding the general nature of the tumor, 34% favoring a mesenchymal origin (chondrosarcoma, chondrofibrosarcoma), 28% for an epithelial origin (with cartilaginous metaplasia), and 38% for a neoplasm with both epithelial and mesenchymal neoplastic components (carcinosarcoma, mixed tumor). This lack of consensus may reflect the unusual morphology and rarity of this case. It was noted during the discussion that this case has not yet completed the NTP peer-review process, so the presenter's diagnostic choice (preputial gland mixed tumor) was not definitive.

The preputial and clitoral glands are homologous, specialized, paired sebaceous glands found, respectively, in male and female mice and rats. Their secretions contain pheromones attractive to the opposite sex (Orsulak and Gawienowski 1972). The glands (8–20 mm long and up to 5 mm wide) are located in the subcutaneous tissue on either side of the base of the external genitalia (Beaver 1960; Hebel and Stromberg 1976; Reznik and Ward 1981). Histologically, the preputial and

clitoral glands are lightly encapsulated, holocrine, branched, tubuloalveolar glands composed of acini supported by a scanty fibrous stroma and lined by flattened, peripheral, basal cells and more central, plump, sebaceous-type cells packed with numerous lipid droplets and bright eosinophilic secretory granules (lysosomes containing acid hydrolases, phospholipids, glycoproteins, and $\alpha_{2\mu}$-globulin) (Beaver 1960; Mancini et al. 1989; Mesquita-Guimarães and Coimbra 1974). The acini empty into branching lateral ducts, which in turn empty into a large central duct, and then into an extraglandular excretory duct. The preputial excretory ducts terminate at the junction of the parietal prepuce and skin, while the clitoral excretory ducts open near the urethra near the distal end of the clitoris (Hebel and Stromberg 1976). Both ducts are lined by stratified squamous epithelium, with keratinization usually only in the excretory duct (Reznik and Ward 1981).

Epithelial neoplasms of the preputial/clitoral glands are uncommon spontaneous lesions in F344/N rats. For example, the incidences of combined adenomas and carcinomas for control F344/N rats in the current (2010) NTP historical control data (HCD) of 1,295 male and 1,247 female F344/N rats (http://ntp.niehs.nih.gov/ [accessed August 2010]) are 5.3% for preputial glands and 12.7% for clitoral glands. Other epithelial neoplasms, such as squamous cell papillomas and carcinomas, are less common in these glands as there are no cases of either in the current NTP HCD. Increased incidences of preputial and/or clitoral gland epithelial neoplasms in male and/or female rats have been considered clear evidence of carcinogenicity in several NTP 2-year carcinogenicity bioassays (NTP 1989, 1990a, 1990b, 1991a, 1991b, 1992, 1993a, 1993b). In most of these studies, the neoplasms were components of multiorgan neoplastic responses caused by potent carcinogens. Mesenchymal-origin tumors of the preputial/clitoral glands are rare spontaneous lesions in F344/N rats, and have not been identified as treatment effects in any NTP studies. In the current (2010) NTP HCD, the only preputial/clitoral gland mesenchymal neoplasms are one case each of fibrosarcoma and sarcoma in female F344/N rats (0.08% incidence for each). An earlier survey of preputial/clitoral gland neoplasia in treated and control F344/N rats noted only 1 preputial gland fibroma (in a treated male) out of 359 clitoral/preputial gland neoplasms examined (Reznik and Ward 1981). Thus, the present case is unusual not only for its mixture of presumably neoplastic mesenchymal (cartilaginous/fibrous) and epithelial (ductal/acinar) elements, but also for the extensive cartilaginous differentiation of the mesenchymal component.

WHAT IS THAT EOSINOPHILIC MATERIAL?

Dr. Susan Elmore (U.S. National Institute of Environmental Health Sciences [NIEHS] and the NTP, Research Triangle Park, NC, USA) presented two cases characterized by accumulation of amorphous, extracellular, eosinophilic material. The first case was in the kidney of pulegone-treated rats and mice, a project done in collaboration with Drs. Jim Morrison and Scott Auerbach. The images presented for voting were from an H&E-stained kidney section in a B6C3F1 mouse that had been treated with 75 mg/kg pulegone by gavage for 2 years (Figures 4A and 4B). The voting choices and results were amyloid (61%), hyaline glomerulopathy (24%), membranous glomerulopathy (4%), fibrillary glomerulopathy (3%), immunotactoid glomerulopathy (3%), glomerulosclerosis (1), and "other" (3%). The NTP diagnosis was hyaline glomerulopathy, a choice made based on a previously published report that used this terminology, but it was not surprising that the majority of the audience voted for amyloid since this lesion has characteristics identical to amyloid on H&E-stained tissues (i.e., the majority of glomeruli contained an eosinophilic material that effaced the mesangium and capillary loops; Figures 4A and 4B). Differentiation between these two entities requires special stains using such traditional methods for identifying amyloid as a Congo red stain using polarized light, Lieb's crystal violet stain, Sirius red stain, and fluorescence microscopy with thioflavine-T (Hobbs and Morgan 1963; Cooper 1969; Brigger and Muckle 1975).

Several essential oils contain pulegone and are used for flavoring foods, drinks, and dental products; as fragrance agents; and in herbal medicines. This study was from an NTP bioassay with male and female F344/N rats and B6C3F1 mice receiving pulegone in corn oil by gavage for 3 months or 2 years (NTP TR 563, http://ntp.niehs.nih.gov/). The doses and groups with renal lesions are listed in Table 1. In the subchronic studies, renal lesions were not evident in mice, but the two highest-dose groups of male rats (2/10 and 10/10) and the highest-dose group of female rats (8/10) had renal lesions characterized by minimal mesangial thickening and occasional clusters of eosinophilic globules (Figures 4C and 4D). Transmission electron microscopy (EM) revealed that globules developed within expanded podocytes (visceral epithelial cells that wrap around the capillaries of the glomerulus; Figures 4E and 4F).

Hyaline glomerulopathy was evident in the 2-year mouse study in all dose groups (Table 1, Figures 4A and 4B). Other lesions included mesangiolysis and intraglomerular hemorrhage. Amyloid was absent as indicated by negative Congo red, Lieb's cresyl violet, and Bennhold's Congo red stains. No immune complex deposition was detected within the basement membranes with Jones's methenamine silver stain, and the material was positive for periodic acid-Schiff (PAS). Increased mesangial matrix and fibrin thrombi were detected with Masson's trichrome. Multiple foci of positive labeling were evident within glomeruli as indicated by IHC detection of IgM, IgG, and IgA, whereas C3 was negative (data not shown). EM revealed electron-dense deposits expanding the mesangium in minimally affected glomeruli with irregular thickening of capillary loop basement membranes as well as podocyte fusion and effacement (Figures 4G and 4H). In glomeruli with marked lesions, the ultrastructural changes included large, well-circumscribed accumulations of closely packed tubules which were nonbranching but curvilinear, occasionally forming swirls (Figures 4I and 4J).

There is one report in the literature of a similar spontaneous rodent lesion that was defined as "hyaline glomerulopathy"

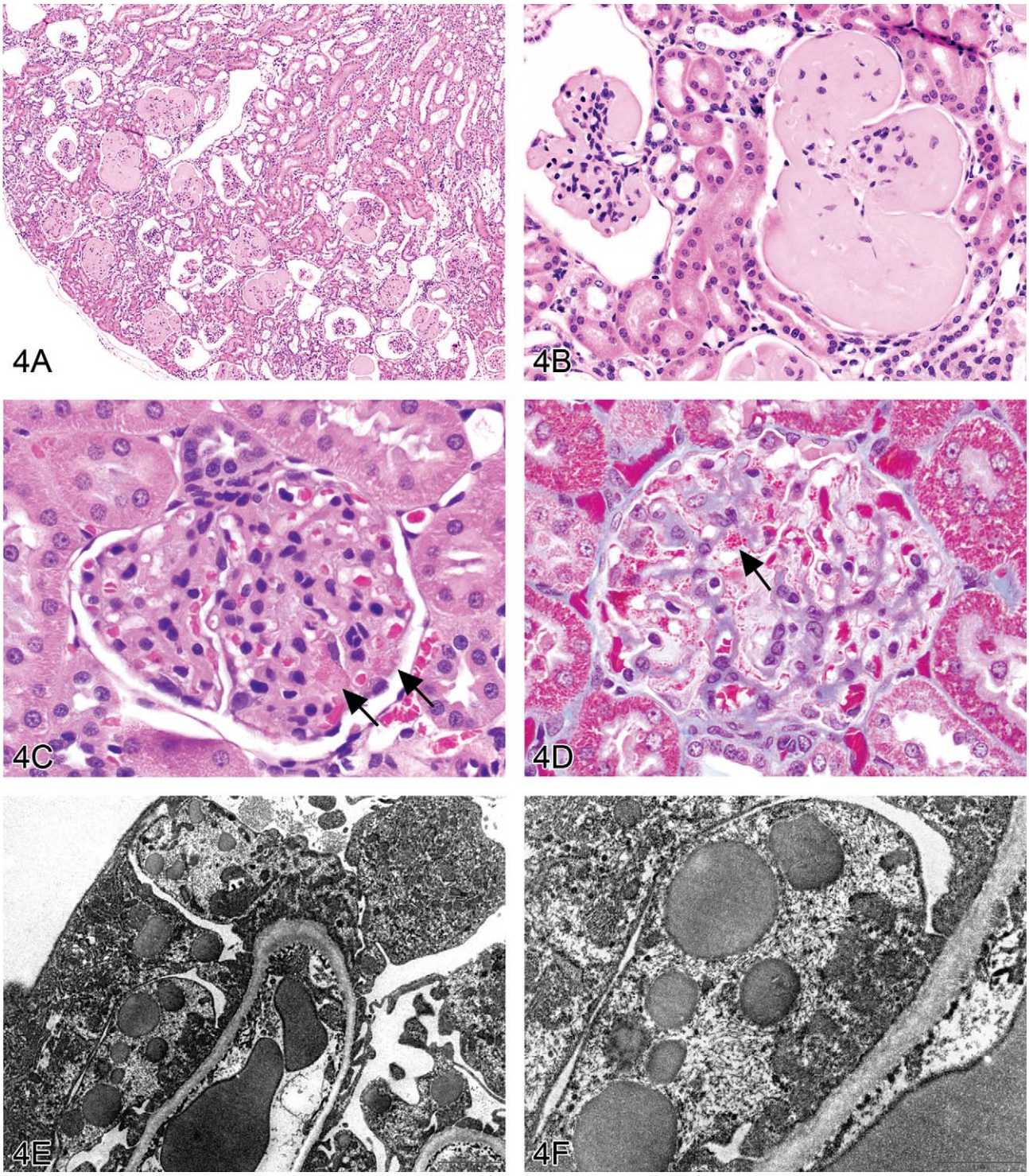

FIGURE 4A–L.—Non-amyloid eosinophilic deposits in the kidney of mice and rats. (A) Low and (B) high magnifications of hyaline glomerulopathy from a B6C3F1 mouse treated with pulegone (75 mg/kg by gavage for 2 years). H&E. The renal glomeruli are expanded by amorphous, extracellular, eosinophilic material that effaces the mesangium and capillary loops. (C) The renal lesion from the rat subchronic (90 days) pulegone study is characterized by minimal mesangial thickening and occasional aggregates of eosinophilic globules within glomeruli (arrows). H&E. (D) The mesangium stains blue (indicating collagen fibrils), whereas the aggregates stain magenta (arrow) with Masson's trichrome stain. (E, F) Transmission electron microscopy (TEM) shows the location of these globules within expanded processes of podocytes. (G) TEM of a glomerular capillary loop from a control animal illustrating the uniform thin basement membrane and typical narrow structure of podocyte processes. (H) TEM of a minimally affected kidney from a mouse in the 2-year study reveals electron-dense deposits (arrows) expanding the mesangium, with irregular thickening of the capillary loop basement membrane as well as podocyte fusion and effacement. (I, J) In a glomerulus with marked lesions, the ultrastructural changes included large, well-circumscribed accumulations of closely packed tubules that are

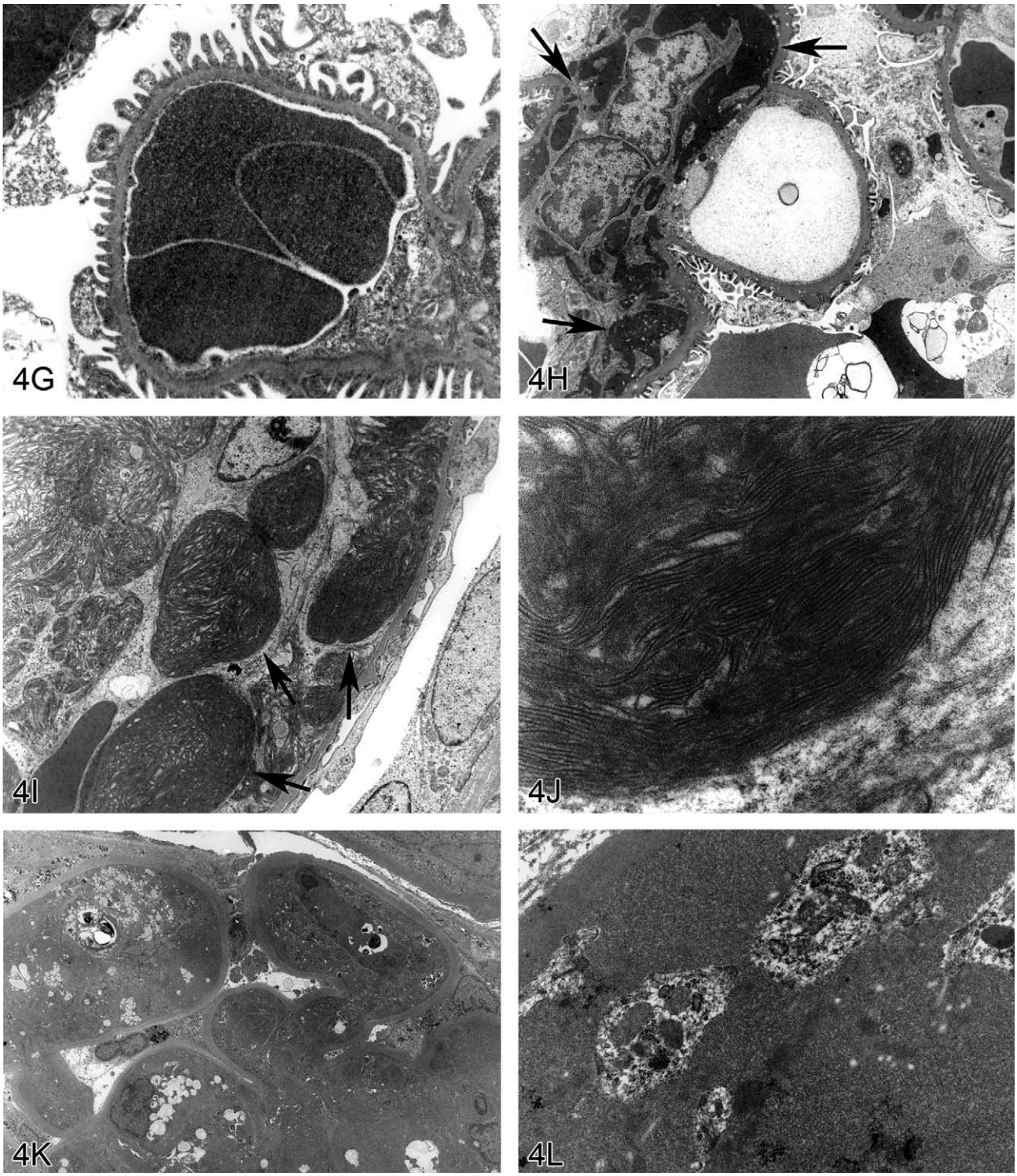

FIGURE 4.—**(continued)** non-branching but curvilinear, occasionally forming swirls. (K, L) In the chronic F344/N rat pulegone study, the lesion has a somewhat different TEM morphology; the glomerular tuft is expanded by an amorphous, finely granular, variably electron-dense material with occasional aggregates of small, smooth-margined vacuoles and entrapped cytoplasmic organelles.

(Wojcinski et al. 1991). The lesion occurred in 2 B6C3F1 mice (out of 920 animals in two carcinogenicity bioassays); the change could not be linked to systemic disease and was not reported as a treatment-related lesion. A similar lesion occurred in transgenic mice engineered to express NNT-1/BSF-3 in the liver under the control of the apolipoprotein E promoter (Senaldi et al. 2002). This is the first literature report of hyaline glomerulopathy in rats, and it is the first in which a chemical treatment (pulegone) was shown to induce this change. The morphology with H&E, PAS, Jones's methenamine silver,

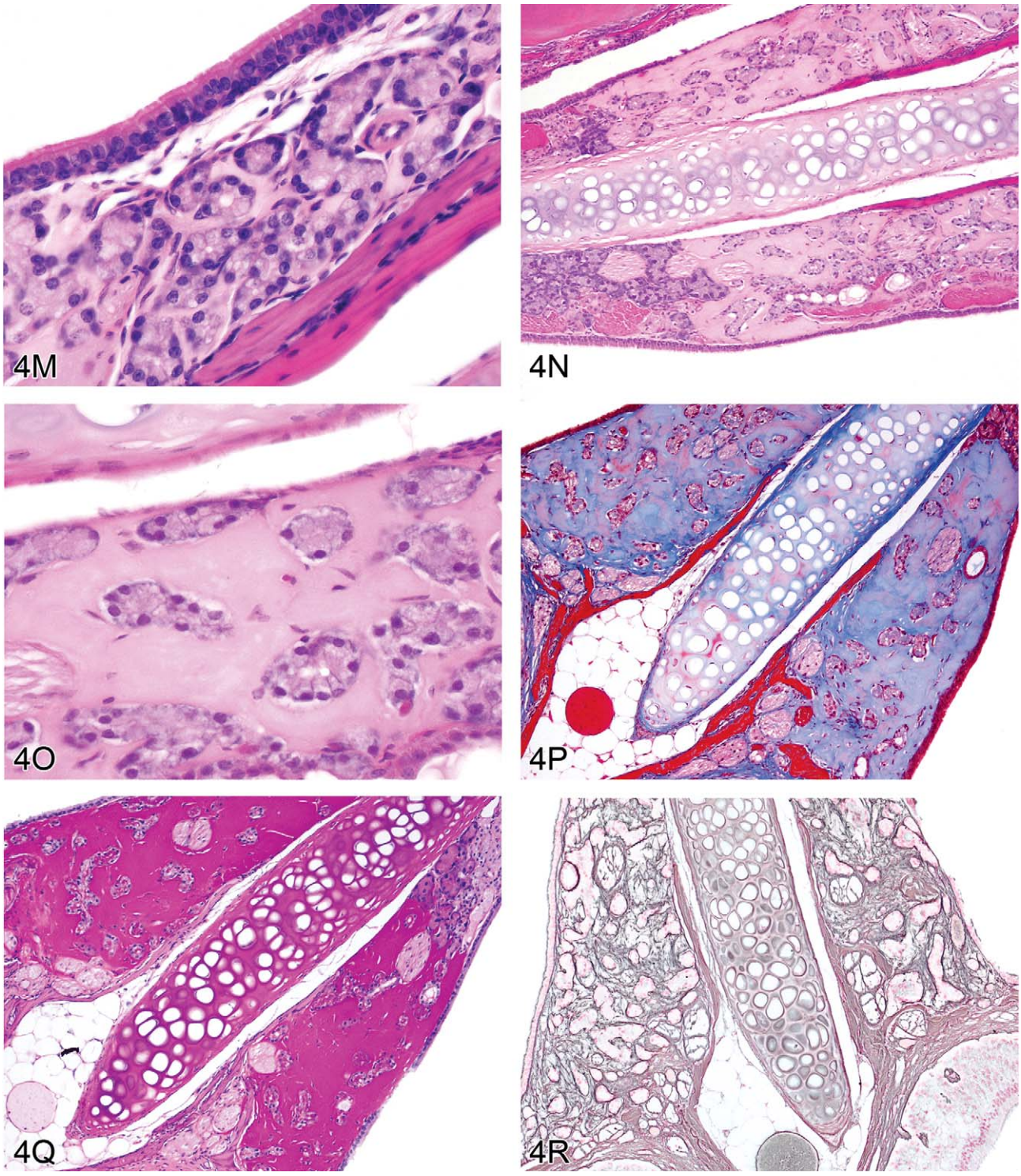

FIGURE 4 M–R.—Non-amyloid eosinophilic deposits of minimal (M) to mild (N, O) degree within the nasal septum at levels I and II from 2-year-old B6C3F1 mice (Herbert and Leininger 1999). H&E. This lesion is characterized by an amorphous and acellular eosinophilic material within the nasal septum that appears to be associated with the nasal glands and the vomeronasal organ. There is no inflammation or degeneration present. This material stains pale blue with occasional red areas with Masson's trichrome (P) and stains dark magenta by the periodic acid-Schiff (PAS) reaction following prior diastase treatment (Q). A silver stain reveals reticulin fibers and occasional disruption of the glandular basement membrane (R).

TABLE 1.—Pulegone study design and results.

3 month male & female mice	0	9.375	18.75	37.5	75	150
3 month male rats	0	9.375	18.75	37.5	75*	150*
					2/10	10/10
3 month female rats	0	9.375	18.75	37.5	75	150*
						8/10
2 year male mice	0	–	–	37.5*	75*	150*
				19/50	30/50	44/50
2 year female mice	0	–	–	37.5*	75*	150*
				3/50	15/50	41/50
2 year male rats	0	–	18.75	37.5*	75*	–
				9/50	24/50	
2 year female rats	0	–	–	37.5*	75*	150*
				17/50	49/50	48/49

Asterisks indicate groups in which hyaline glomerulopathy was observed in renal glomeruli. A dash indicates no dose. When the lesion was present, the incidence is indicated. Due to excessive morbidity and mortality, males given 75 mg/kg and females given 150 mg/kg did not receive pulegone after week 60 (stop-exposure), but instead were treated with corn oil vehicle until the end of the study.

Masson's trichrome, and Congo red stains in F344/N rats was similar to that observed in mice. This glomerular lesion was also negative for C3 but multifocally positive for IgM, IgG, and IgA (data not shown). By EM, glomerular tufts were expanded by an amorphous, finely granular, variably electron-dense material with occasional aggregates of small, smooth-margined vacuoles and entrapped cytoplasmic organelles (Figures 4K, 4L).

Hyaline glomerulopathy in mice and rats has similar morphological features to the human condition of immunotactoid glomerulopathy (IG) (Schwartz 2007). IG is characterized by mesangial expansion with eosinophilic, PAS-positive material. Deposits may be slight to massive; glomerular distortion occurs in the latter case. As in mice and rats, this material is blue with trichrome stain and negative with Congo red. There is variable positivity with IgG, IgA, IgM, and C3. By EM, the fibrils or tubules are elongated and nonbranching, but the appearance of the fibrils and the state of organization can vary from case to case. IG is not associated with systemic disease, and the etiology and pathogenesis are unknown.

The second case presented by Dr. Elmore was a collaborative effort with Dr. Pamela Blackshear and involved a spontaneous lesion in the nasal septum at levels I and II from 2-year-old B6C3F1 mice. Voting choices and results based on several images (Figures 4M, 4N, 4O) were hyalinosis (37%), interstitial hyalinosis (27%), amyloid (15%), eosinophilic substance (11%), nasal gland secretion (5%), nasal gland proteinosis (5%), and "other" (0%). These mice were from an NTP chronic bioassay, and the lesion was present in most mice in the study (both controls and treated) with a range of severity. This lesion was characterized by deposition of an amorphous and acellular, eosinophilic material within the nasal septum and appeared to be associated with the nasal glands and vomeronasal organ, but there was no inflammation or degeneration present. A Congo red stain was done because the historical diagnosis for this lesion is amyloid; however, no amyloid was detected (Herbert and Leininger 1999; Renne et al. 2009). This material stained pale blue with occasional red areas with Masson's trichrome and was dark magenta by PAS with prior diastase treatment (Figures 4P, 4Q). Similar PAS-positive material occurred within seromucous nasal glands. In animals with a moderate or marked amount of PAS-positive interstitial material, deposition within the glands was decreased. Similarly, when there was no or minimal interstitial material, the amount within the glands was increased (data not shown), suggesting a connection between these two sites. A reticulin stain revealed reticulin fibers and occasional disruption of the glandular basement membrane (Figures 4R).

This lesion has been previously diagnosed as "eosinophilic substance" (ES) (Doi et al. 2007, 2009, 2010). Present within the mouse nasal septum, it increases in volume with age (which plateaus over time), is more intense in males, and is not associated with degeneration or inflammation. Similar to the current investigation, the material was Congo red-negative, PAS-positive with prior diastase treatment, and pale blue with occasional red areas by Masson's trichrome. Reticulin and collagen fibers were sparse in the areas that were pale red in trichrome-stained material. Electron microscopy showed the absence of nonbranching fibrils consistent with amyloid, instead revealing amorphous deposits in the interstitium as well as accumulation within and near the rough endoplasmic reticulum of nasal gland epithelial cells. These findings suggest that this material arises as a secretory product from the nasal gland epithelial cells.

After presentation of the full case file, a revote resulted in the following choices: nasal septum hyalinosis (52%), eosinophilic substance (21%), interstitial hyalinosis (14%), nasal gland secretion (5%), nasal gland proteinosis (5%), "other" (3%), and amyloid (0%), indicating that many individuals had changed their minds—including all people who originally elected amyloid. The take-home message is that "not everything that is eosinophilic, amorphous, extracellular, and acellular is amyloid!"

A BRIEF INTRODUCTION TO PROPOSED INHAND NOMENCLATURE FOR PROLIFERATIVE LESIONS OF THE CNS/PNS

The International Harmonization of Nomenclature and Diagnostic Criteria for Lesions in Rats and Mice (INHAND) initiative is a collaboration of the societies of toxicologic pathology in Europe, Japan, and North America to develop a consensus of preferred terms to use for spontaneous proliferative and nonproliferative changes, mainly of a spontaneous nature, in rats and mice (http://www.toxpath.org/inhand.asp). A Global and Editorial Steering Committee (GESC) oversees the activities of this project and is composed of toxicologic pathologists from all the participating societies. Working groups for each organ system are the core of the project, and are responsible for the publication of updated nomenclature (with representative images) for each system.

Dr. Alys Bradley (Charles River Laboratories, Tranent, Edinburgh, UK), the GESC member representing the British Society of Toxicological Pathologists (BSTP) and a member of the INHAND Nervous System Working Group, provided a list of terms for proliferative lesions that are currently under

consideration. Of this list, Dr. Bradley gave detailed information on proposed terminology for multiple CNS and PNS neoplasms, picking one case from a high-dose CD-1 mouse from a 2-year study (Figures 5A–F) to present and discuss in detail. Voting choices and results were malignant ependymoma (40%), malignant medulloblastoma (21%), choroid plexus carcinoma (19%), malignant astrocytoma (10%), benign ependymoma (10%), benign schwannoma (0%), and malignant schwannoma (0%). Malignant ependymoma was the correct choice. Differential diagnoses for this neoplasm are choroid plexus carcinoma and malignant medullublastoma.

Ependymal cells are cuboidal, ciliated cells that line the cerebral ventricles and central canal of the spinal cord and have essential roles in brain homeostasis and transport of cerebrospinal fluid. The ependyma, as well as the majority of neurons, astrocytes, and oligodendrocytes, arise from mitotically active, multipotent progenitor cells termed radial glia. Histologically similar ependymomas from different parts of the CNS represent molecularly and clinically distinct neoplasms that arise from different populations of radial glia stem cells. Thus, different ''populations'' of ependyma are unlikely to respond uniformly to all treatments (Taylor et al. 2005; Poppleton and Gilbertson 2007)

In domestic animals, ependymomas are uncommon tumors that can arise from the ventricular system along the entire craniospinal axis. Most are observed in dogs and cats, but they have also been reported in cattle and horses. Luminal rosettes formed of ciliated cells, a major diagnostic feature of these tumors, are more commonly seen in feline and human ependymomas. Grossly these neoplasms are soft, and grey or red if hemorrhagic. Expansion into the ventricular space can result in obstructive hydrocephalus. Ependymomas are rare tumors in the CNS of rats and mice (Table 2). Rodent ependymomas lack luminal rosettes, but they do contain foci of capillary endothelial proliferation that are not present in human ependymomas. Human ependymomas have other unique cytoarchitectural features such as vacuoles and papillary projections. Tanycytic ependymoma in humans is an uncommon fibrillar variant of ependymoma that originates from ventricular sites, most commonly the spinal cord, and is characterized by streams of piloid, or hair-like, cells having ''ependymal'' nuclei. Tanycytes (stretch cells) are specialized ependymal cells found most commonly at the circumventricular organs, including the floor of the third ventricle, and have long basal processes projecting into adjacent nervous tissue. True ependymal rosettes are absent, and perivascular rosettes are inconspicuous in tanycytic ependymomas. The tumor, easily confused with pilocytic astrocytoma, is best identified by its characteristic ultrastructural features, which include numerous microvilli and intracytoplasmic microtubules (Langford and Barré 1997). Tanycytic ependymomas have not yet been reported in rodents.

Concluding her talk, Dr. Bradley provided helpful tips concerning special techniques for diagnostic evaluation of ependymomas. These included the following expression patterns for various neural cell type-specific markers:

- Human neoplasms express vimentin and may express the glial cell marker glial fibrillary acidic protein (GFAP).
- Rodent neoplasms usually express vimentin but little or no GFAP.
- Vimentin is expressed in neurons during embryonic development.
- Mouse ependymal cells express S100β and L-glutamate/L-aspartate transporter (GLAST).
- Blepharoplasts (derivatives of centrioles) may be identified in ependymomas using phosphotungstic acid–hematoxylin (PTAH) stain.

An Introduction to INHAND nomenclature of CNS/PNS Nonproliferative Lesions with Examples of Diagnoses

The next speaker, Dr. Jenny McKay (AstraZeneca, Macclesfield, UK), Chair of the INHAND CNS Nervous System Sub-Group responsible for the nomenclature of nonproliferative lesions in rodents, provided an update focusing on diagnoses that had provoked considerable discussion within the working group. The term ''vacuolation'' was presented with an emphasis on the importance of identifying the anatomical location of this change. An example of white matter vacuolation or ''intramyelinic edema'' induced by triethyltin was shown (Figure 6A), together with the proposed INHAND synonyms, histogenesis, microscopic diagnostic features, and differential diagnoses. This change was contrasted with the appearance of grey matter vacuolation (Figure 6B) and artifactual vacuolation (Figure 6C). There was a lively audience discussion on the subject of artifactual vacuolation and the difficulties regarding its interpretation, especially if it is just confined to high-dose animals. One participant described a study with mucocytes in high-dose animals only. Another highlighted the rat optic nerve and medulla oblongata as common sites of vacuolation due to procedural problems during necropsy. Extended holding (over the weekend) of CNS samples in the 70% ethanol bath of automated histology processors was another issue for some laboratories. It was suggested that special stains, careful recording of lesions between groups, and more accurate recording of the processing conditions could all help to distinguish artifact from real vacuoles. Following this discussion at the satellite symposium, the INHAND subgroup on nonproliferative neural lesions decided to add a section on commonly encountered artifacts—including vacuoles—to the INHAND document on neural nomenclature.

The discussion moved next to consider a series of terms for reactive changes in the nervous system. ''Demyelination'' combines vacuolation with inflammation, gliosis, and/or axonal degeneration. Glial responses can be defined using a number of terms: the cell type-specific terms ''astrogliosis'' and ''microgliosis,'' the catchall category ''gliosis,'' and the location-related ''satellitosis.'' These designations can usually be made on H&E sections (e.g., increased eosinophilic cytoplasm, eccentric nuclei, and swollen processes in the case of ''astrogliosis''); the application of commercially available IHC markers enables more precise identification of glial cell types. The final term

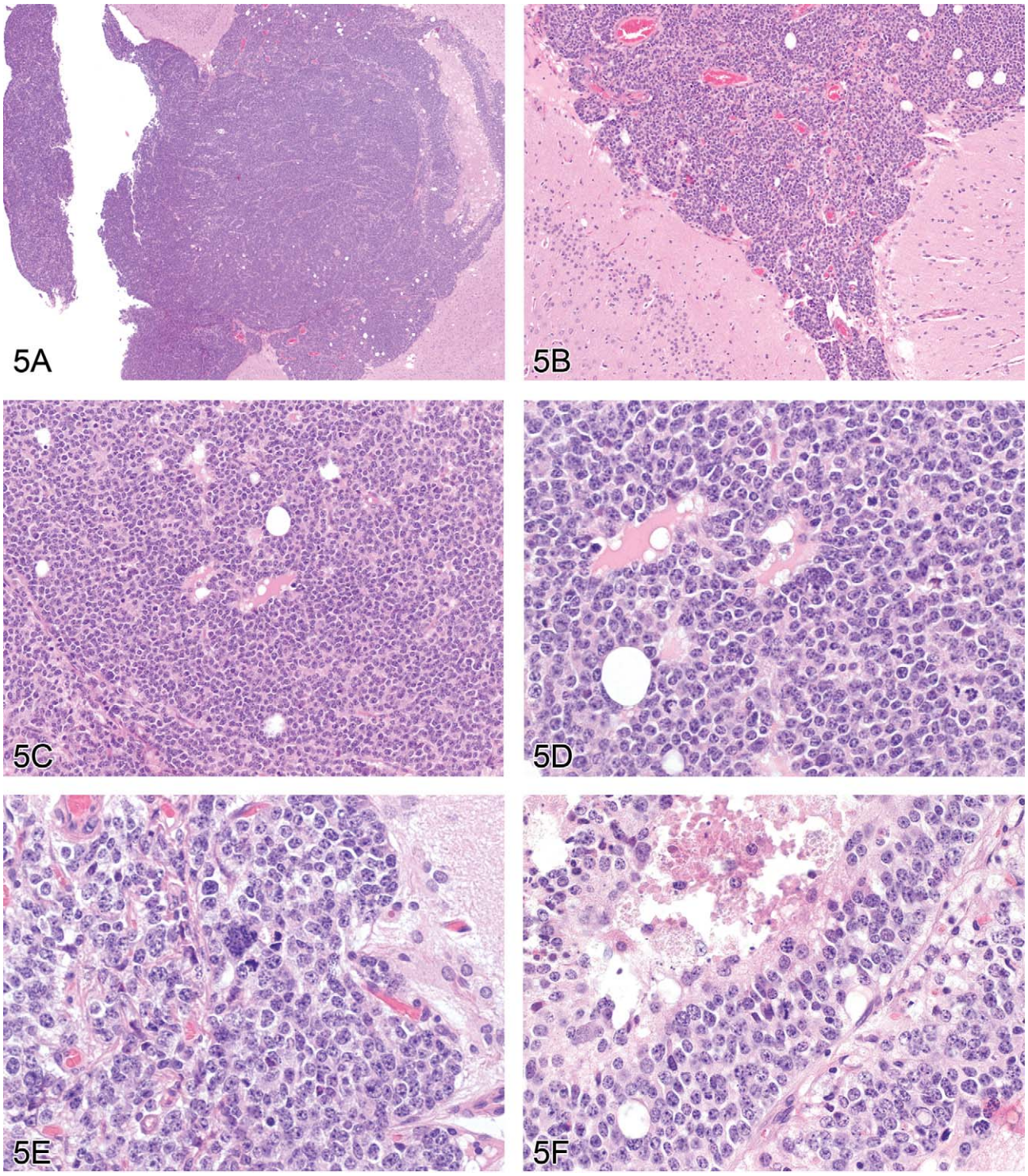

FIGURE 5.—(A–F) Malignant ependymoma in a mouse. A series of images presented for voting from a CD-1 mouse in a high-dose group from a 2-year study. The lesion exists as a round cell tumor in proximity to the ventricular system. Differential diagnoses include choroid plexus carcinoma and malignant medulloblastoma. H&E.

discussed was "axonal degeneration," which the INHAND working group agreed should be the preferred generic description when a cause cannot be established. Alternative terms have specific uses because they imply a given pathogenesis. For example, "axonopathy" implies primary damage to the axon with pathologic loss of distal axons but survival of the nerve cell body, and "Wallerian degeneration" implies that the distal axon has been severed from the central components by surgical or chemical transection. In this manner, the audience was reminded that such specific designations should only be used

TABLE 2.—Incidence of rat and mouse ependymomas.

Rat ependymomas
Ward and Rice (1982) surveyed F344 rats and found that ependymomas comprised 4% of the total brain tumors recorded.
Maekawa et al. (1984) surveyed 692 F344/DuCrj and 377 Wistar rats and found no ependymomas diagnosed.
Krinke et al. (1985) surveyed 8,960 Sprague-Dawley rats and found 2 ependymomas recorded (2% total brain tumors).
Gopinath (1986) surveyed 5,395 Sprague-Dawley rats and found 1 ependymoma recorded in a male rat (1% total brain tumors).
Yamate et al. (1987) surveyed 3,410 F344 rats and found 2 ependymomas diagnosed (2% total brain tumors).
Giknis and Clifford (2000) surveyed 3,377 Sprague-Dawley rats and found no ependymomas diagnosed.
Inveresk/Charles River Edinburgh Background incidences (1998–2009) surveyed 2,437 Sprague-Dawley rats and found 1 ependymoma diagnosed.[a]
Mouse ependymomas
Radovsky and Mahler (1999) surveyed 4,894 B6C3F1 mice from the NTP archives and found no ependymomas diagnosed.
Fraser (1986) surveyed 75,000 mice from the Edinburgh MRC Neuropathogenesis unit archives (strains: A2G/LacDk, VM/Dk, MB/Dk, PCD, C57BL/FaDk, LM/Dk, MM/Dk, SM/RrDk, BALB/c/LacDk, BRVR/SrDk, C3H/LacDk, BSC/Dk, DBA/2LacDk, NZB/LacDk, RIII/FaDk, VM, MB, IM) and found no ependymomas diagnosed.
Mikaelian et al. (2004) surveyed 9,284 mice from the Jackson Lab archives (strains C57BL6/J, 129P3/J, A/J, BALB/cByJ, BALB/cJ, C3H/HeJ, CBA/J, DBA/2J, HRS/J, SJL/L) and found no ependymomas diagnosed.
Giknis and Clifford (2000) surveyed 5360 Crl:CD-1 (ICR)BR Mice and found 1 ependymoma recorded in a female (1% total brain tumors).
Inveresk/Charles River Edinburgh Background incidences (2002) surveyed 1,851 Crl:CD-1 (ICR)BR Mice and found 1 ependymoma diagnosed.[a]
Charles River Edinburgh Background incidences (2010) surveyed 5,755 Crl:CD-1 (ICR)BR Mice and found 1 ependymoma diagnosed.[a]

[a] Unpublished data from Inveresk/Charles River Laboratories, Edinburgh, UK.

when communicating the pathogenesis of axonal degeneration, but they are not morphologic descriptors in themselves.

Dr. McKay ended by presenting a sciatic nerve lesion in a 13- to 15-week-old Lewis rat (Figures 6D–6F). The voting choices based on nerve images processed using Luxol fast blue or IHC techniques to reveal axonal processes and macrophages were (1) axonal degeneration, (2) demyelination, (3) axonal degeneration with demyelination, (4) Wallerian degeneration, and (5) Wallerian-type degeneration. The audience preferred axonal degeneration with demyelination (70%), which was in line with Dr. McKay's recommendation since she had not revealed the cause of the axonal degeneration. After voting was completed, the pathogenesis was revealed to be a chronic constriction injury (Bennett and Xie 1988) in which one nerve was loosely ligated with chromic gut sutures so that inflammation-associated nerve swelling would eventually axotomize the compressed fibers (in effect producing "Wallerian-type" degeneration). Without prior knowledge of the cause, however, the correct diagnostic term would be the most generic designation denoting axonal injury. An audience member asked whether IHC for ED-1 (a marker for activated rat microglia, monocytes, and macrophages) was labeling Schwann cells or macrophages in damaged nerves. The following discussion confirmed that the PNS inflammatory response is evaluated using ED-1 to label macrophages and S100 to demonstrate Schwann cells (Takahashi et al. 2004).

RETINAL GLIOSIS

Dr. Deepa Rao (NIEHS and the NTP, and Integrated Laboratory Systems, Inc., Research Triangle Park, NC, USA) began the afternoon session with a case titled "The Eyes Have It." This project was conducted in collaboration with Drs. Susan A. Elmore, David E. Malarkey, James P. Morrison, and Peter B. Little. Photomicrographs of a retinal lesion were shown from a control F344/N rat in a 2-year NTP bioassay at terminal necropsy. Voting results were well distributed across seven voting choices: retinal gliosis (36%), spindle cell proliferation (17%), ectopic nerve bundles (16%), retinal glioma (12%), malignant schwannoma (9%), retinal hyperplasia (5%), and "other" (5%). The subsequent presentation detailed the species-specific differences in retinal gliosis between rodents and humans. Unlike rodents (Yoshitomi and Boorman 1990), human cases are typically expansive and often termed "massive gliosis of the retina" (Yanoff, Zimmerman, and Davis 1971).

Normal structures within the optic nerve fiber layer include optic nerve fibers (which are axons from the ganglion cells) coursing toward the optic disc, traversing glial processes of the Mueller cells that extend to the inner limiting membrane via foot processes and possible astrocytes aligned parallel to the nerve fibers. Routine H&E-stained sections demonstrate that rodent retinal gliosis was focal, localized around the optic disc area, and confined within the optic nerve layer (Figure 7A) without breaching the overlying inner retinal membrane or invading the underlying ganglion cell layer or inner plexiform layer. Cells of interest uniformly expanded the optic nerve layer (Figure 7B), often as aggregated foci, and had ovoid nuclei, abundant fibrillar cytoplasm, indistinct cell borders, and rarely had mitotic figures (seen in 1/14 cases). A few scattered, dilated blood vessels associated with the lesion were commonly present. The origin of cells in rodent cases of retinal gliosis remains unconfirmed (Guess What! ESTP Case 5, at http://www.eurotoxpath.org/guesswhat/index.php?id=case5 [accessed March 17, 2010]; Yoshitomi and Boorman 1990). Modern IHC techniques allow histogenesis to be investigated using a panel of markers (Table 3). In the current case, anti-GFAP revealed reactive Müller cells within the site of interest (Figure 7C), but not the specific cells characterizing the retinal lesion. Vimentin labeling was limited to Müller cells (Figure 7D), indicating that the cells of interest were unlikely to arise from this lineage. Neuron-specific enolase (NSE) was evident in the nerve fibers and S100 in glia within the site of

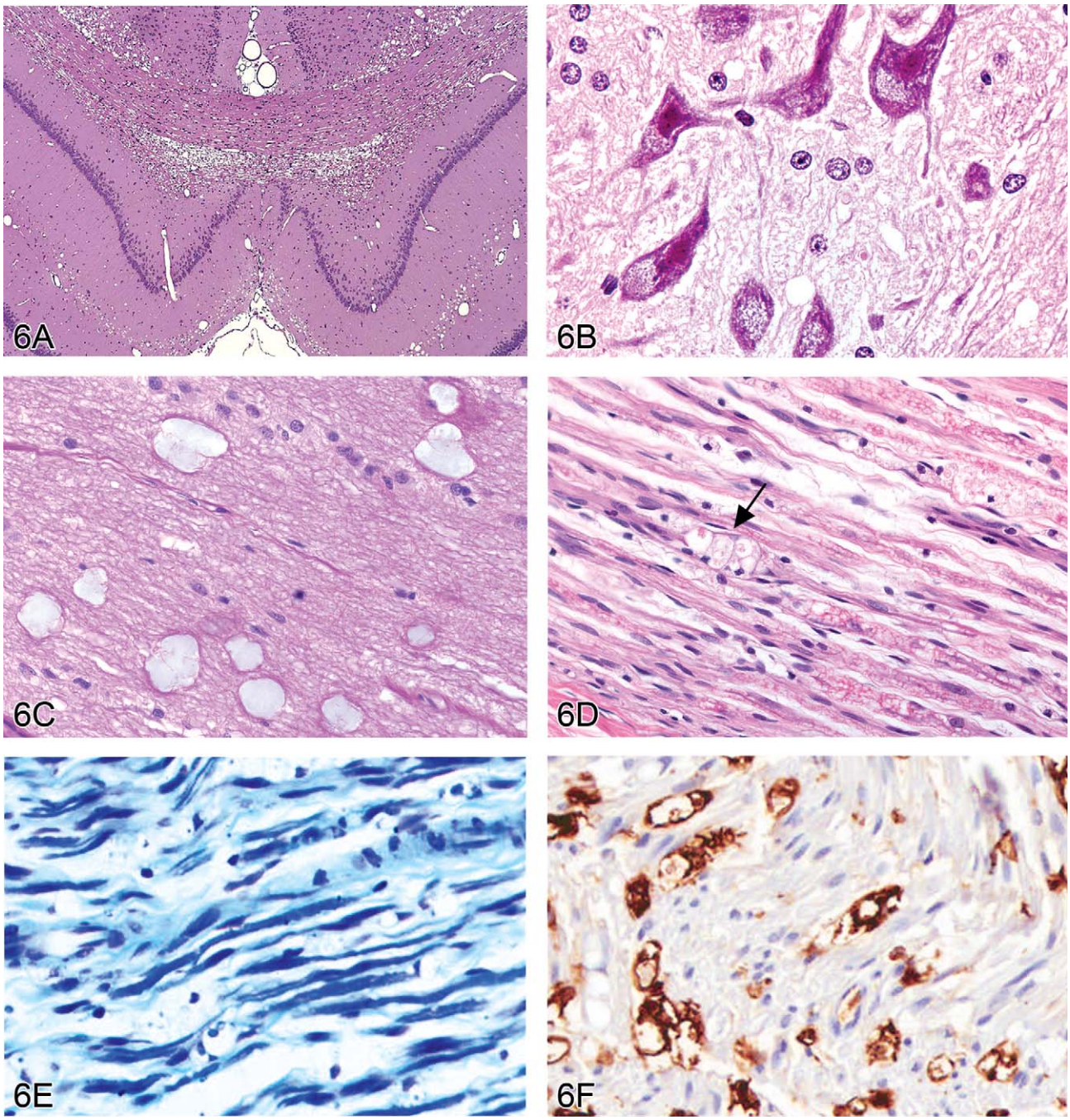

FIGURE 6.—Vacuolar lesions in the nervous system of rodents. (A) Intramyelinic edema in the dorsal hippocampus of the brain of a rat treated with triethyltin. Large numbers of vacuoles are present within the dorsal hippocampal commissure, the corpus callosum and the cingula. H&E. (Image is courtesy of Dr. Robert H. Garman, Consultants in Veterinary Pathology, Murrysville, PA.) (B) Compound-induced foamy cytoplasmic vacuolation in the spinal cord ventral horn motor neurons of a rat resulting from phospholipidosis (confirmed using electron microscopy). H&E. (Image is courtesy of Dr. Anna-Lena Berg, Safety Assessment, Pathology, AstraZeneca, S-151 85 Södertälje, Sweden.) (C) Mucocytes ("Buscaino bodies") in the optic nerve of a dog. These are a common processing artifact associated with extended immersion in ethanol during paraffin infiltration (typically by over-the-weekend holding on an automated processor) and manifest as pale, blue-gray, amorphous bodies in H&E-stained sections. H&E. They are positive for periodic acid-Schiff (PAS), are birefringent under polarized light, and probably represent degraded myelin. (D) Sciatic nerve injury in a Lewis rat. Axons are disrupted as indicated by digestion chambers (arrow), with multifocal myelin fragmentation. H&E. (E) Luxol fast blue stain of sciatic nerve injury in a Lewis rat. When compared to a contralateral control nerve, there is a marked reduction in staining for myelin sheaths. (F) Labeling to demonstrate ED-1 (a rat macrophage marker) of the same sciatic nerve reveals numerous positive macrophages in demyelinated areas. (Images D, E and F are courtesy of Dr. Karima Kahlat, Department of Physiology and Pharmacology, School of Medical Sciences, University of Bristol, United Kingdom.)

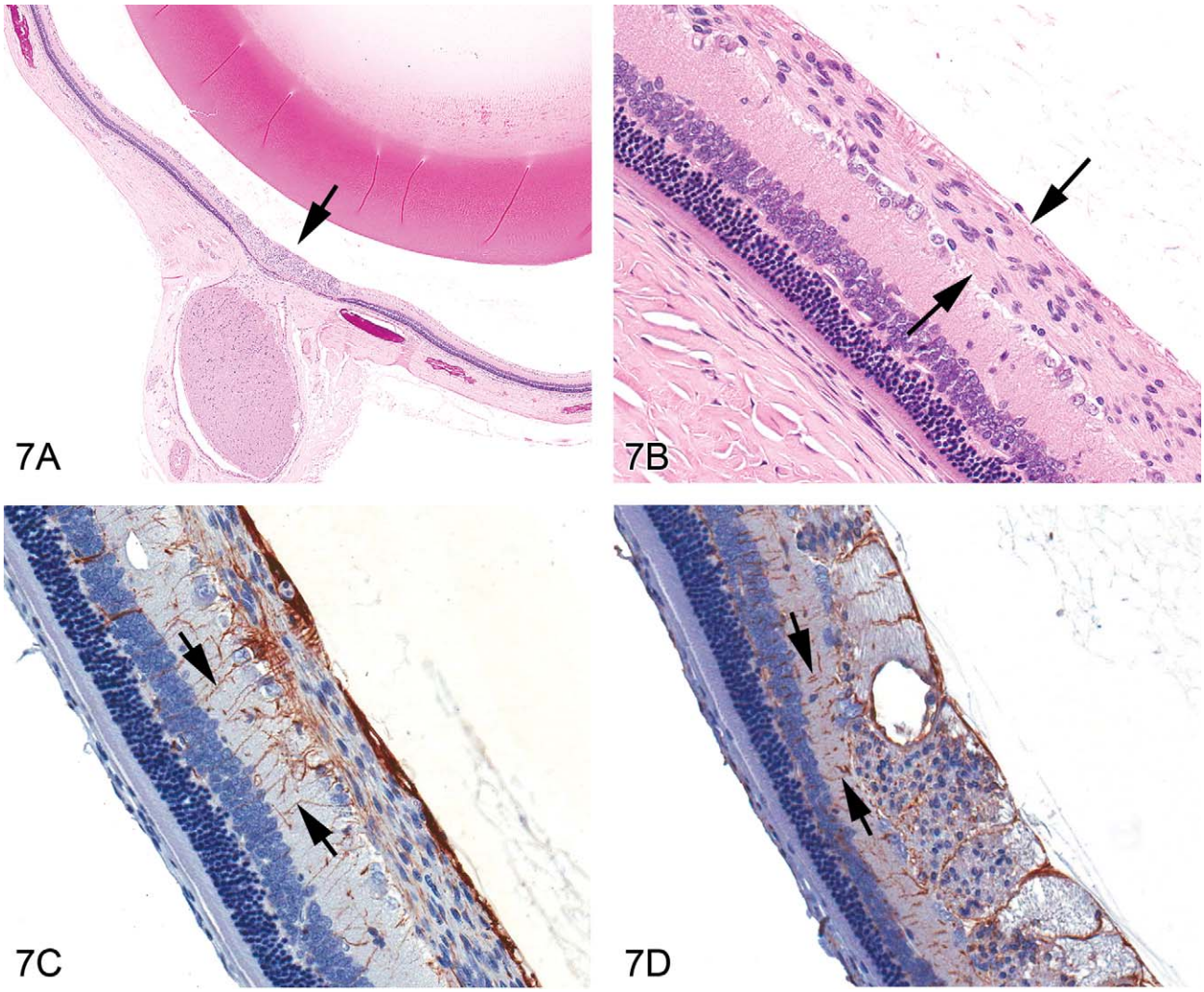

FIGURE 7.—Retinal gliosis in a control F344/N rat. (A) Focally extensive hypercellular lesion (H&E stain) centered within the retina at the optic disc area (arrow). (B) Higher magnification of the lesion showing an expanded optic nerve fiber layer containing cells with elongated nuclei (arrows); fibrillar, eosinophilic cytoplasm; and indistinct cell membranes. (C) Labeling with anti-glial fibrillary acidic protein (GFAP) reveals glial processes (arrows) of reactive Müller cells extending from the outer plexiform layer through the inner nuclear layer and inner plexiform layers abutting the inner limiting membrane. GFAP-stained cells within the optic nerve fiber layer were concluded to be those of traversing Müller cells as well as astrocytes (parallel to the optic nerve fibers), and not the proliferating cells of interest, due to the meager staining immediately adjacent to the nuclei of the cells forming the lesion. (D) Staining with vimentin also clearly identifies glial processes (arrows) of Müller cells and processes within the plexiform, inner nuclear, and optic nerve fiber layers, and inner limiting membrane. Cross-section of the area of interest within the optic nerve fiber layer shows scattered punctate, nonspecific, positive staining with vimentin that was not interpreted to identify the cells of interest.

interest, but not in the specific cells. Taken together, IHC reveals reactive glial cells within the lesion, but could not definitively identify the cell type of interest.

One audience member indicated that this lesion may be compound-related in rats, but in this study it was found in both control and treated rats, and was thus considered to be incidental. Open discussion following the presentation included a proposed diagnosis of "epiretinal membrane" seen in humans. However, because the lesion is confined entirely within the retina in all rodent cases examined, this diagnosis was not considered to be a suitable alternative (in consultation with Dr. Thomas Bouldin, University of North Carolina at Chapel Hill, School of Medicine). The role of ophthalmologic examinations in diagnosing this lesion could not be addressed since the change was only identified during histopathology; no ocular examinations were conducted during the course of the study. Thus, the working diagnosis for such lesions in NTP studies remains "retinal gliosis" at this time.

AN UNUSUAL PROLIFERATIVE DERMAL LESION IN RATS

Dr. E. Terence Adams (Experimental Pathology Laboratories, Inc., Research Triangle Park, NC, USA) presented three cases of an unusual, incidental skin mass identified in F344/N rats

TABLE 3.—Immunohistochemical markers for retinal gliosis.

Immunohistochemical marker	Cell of interest	Staining characteristics
Glial fibrillary acidic protein (GFAP)	Astrocytes and Müller cells	Positive for reactive Müller cells
Ionized calcium binding adaptor molecule 1 (Iba-1)	Microglial cells	Negative
Oligodendrocyte lineage transcription factor 2 (Olig 2)	Oligodendrocytes	Negative
S100	Schwann cells and astrocytes	Positive for astrocytes, not cells of interest
Neuron-specific enolase (NSE)	Neuronal cells	Positive for extracellular optic nerve fibers
Ki67	Cell proliferation	Negative
Vimentin	Mesenchymal cells	Positive for Müller cells only

during the Quality Assessment review of separate NTP chronic studies. The location of the masses included the right thorax, left abdomen, and tail. Voting choices and the results included (1) fibroma with sebaceous hyperplasia (13%), (2) fibroadnexal hamartoma (44%), (3) sebaceous trichofolliculoma (32%), (4) sebaceous adenoma (0%), (5) keratoacanthoma with sebaceous hyperplasia (6%), and (6) other (5%). The histomorphologic features of this rat lesion were consistent with fibroadnexal hamartoma as it has been described in dogs. The multinodular masses had multiple, centrally located, variably sized cavities lined by squamous epithelium and bordered by numerous mature sebaceous glands (Figures 8A and 8B). Many cystic structures had intraluminal amorphous material consistent with sebaceous secretion or segments of hair shaft. Surrounding these folliculosebaceous units were dense bands of mature connective tissue and proliferative fibroblasts (Figure 8B). There was no discernable evidence that folliculosebaceous units opened to the surface. Review of the rodent lesion by several pathologists, including a dermatopathologist, generally supported the diagnosis. However, it was suggested during both the review process and the audience discussion that one of the cases may have been a sebaceous adenoma encircled by an exuberant reactive fibrosis. Another point of contention among several pathologists regarded whether the cystic structures might represent dilated hair follicles or sebaceous ducts.

This is the first report of fibroadnexal hamartoma in rats. Quality assessment review of chronic rat studies in this laboratory suggest that these lesions have been previously diagnosed as fibroma despite the presence of proliferative sebaceous glands and cystic follicular structures. Similar microscopic features have been described in the canine fibroadnexal hamartoma (also referred to as fibroadnexal dysplasia, focal adnexal dysplasia, adnexal nevus, or organoid nevus) (Gross et al. 2005) and in a similar human lesion termed folliculosebaceous cystic hamartoma (FCH) (Kimura et al. 1991; Ramdial, Chrystal, and Madaree 1998). Differential diagnoses for fibroadnexal hamartoma are provided in Table 4. Both fibroadnexal hamartoma (canine) and FCH must be differentiated from sebaceous trichofolliculoma, which is also a cystic follicular mass with an abundant sebaceous component. However, sebaceous trichofolliculoma generally develops as a depressed lesion with a surface opening and lacks the exuberant mesenchymal component observed in fibroadnexal hamartoma and FCH.

PULMONARY VASCULAR LESION IN A MOUSE

Dr. Monique Y. Wells (Toxicology/Pathology Services, Inc., Paris, France) presented a pulmonary vascular lesion in a mouse that was discussed by the INHAND Working Group for nomenclature of non-neoplastic lesions in the cardiovascular system. (The case was submitted to the working group by Dr. Yoshimasa Okazaki.) Dr. Wells first presented the phenotypic characteristics of the MnSOD (manganese superoxide dismutase; SOD2) mouse in which the lesion was found (The Jackson Laboratory, http://jaxmice.jax.org/strain/002973.html [accessed June 15, 2010]) followed by images of the lesion (Figures 9A and 9B). The choices and results were (1) intimal fibrous plaque (41%), (2) organizing thrombus (13%), (3) intramural plaque (19%), (4) arteriosclerosis (3%), (5) intimal cushion (17%), (6) leiomyoma (4%), and (7) "another diagnosis" (3%). The INHAND committee's working diagnosis for this lesion was intramural plaque.

The lesion consisted of a granular, amorphous material with a spindloid cell component located between the endothelium and the tunica media of the affected vessel. A small focus of similar material was evident between the tunica media and the tunica adventitia. Previous publications have used the term "arterial plaque" as the diagnosis (Rehm, Wcislo, and Deerberg 1985; Ernst et al. 1996) and postulated that it represents an organizing thrombus. However, features of the lesion differ from those of compound-related organizing thrombi in pulmonary arteries (Ramot et al. 2010). Another nuance in the interpretation is to clearly identify the vessel of origin, as two kinds of blood vessels coexist in the lung: pulmonary and bronchial (Best and Heath 1961; Kay 1992). The INHAND working groups for the Cardiovascular System and the Respiratory System worked together to ascertain that the lesion involved a pulmonary artery based on several morphologic traits: pulmonary vessels have thin walls in relation to the diameter of the vessel lumen, while bronchial vessels have thick walls and relatively small diameters; the absence of cardiomyocytes in the vessel wall, which is a characteristic feature of pulmonary veins (Figure 9C); and location of the vessel in the interstitial tissue between lung lobes instead of within or closely applied to the wall of a bronchus.

This case promoted considerable discussion from the audience. Comments ranged from concern about the use of the term

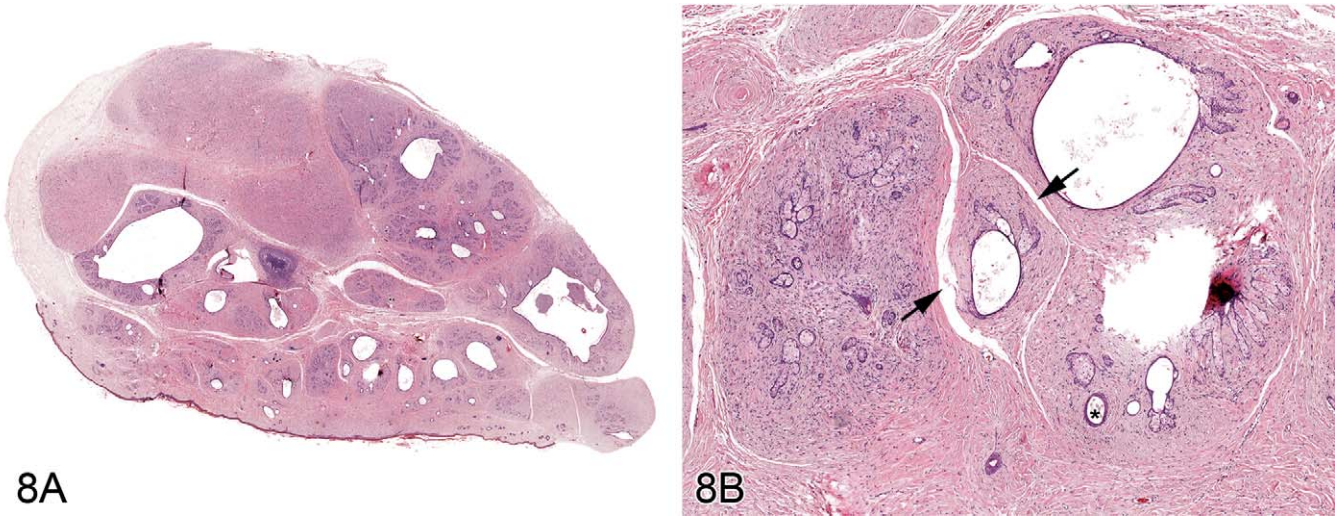

FIGURE 8.—Fibroadnexal hamartoma in a rat. (A) Low magnification of a skin from a F344/N rat. Note the multinodular presentation with distinct folliculosebaceous units (with centrally located cystic follicular structures bordered by abundant sebaceous epithelium) that are separated by a dense collagenous stroma and do not open to the surface. (B) Higher magnification of (A). Folliculosebaceous units with intraluminal sebaceous secretion, hair shafts (asterisk), and cleft formation (arrowheads). H&E.

TABLE 4.—Histologic differential diagnoses for fibroadnexal hamartoma.

Differential diagnosis	Similar features	Different features
Keratoacanthoma (''Infundibular Keratinizing Acanthoma'')	Follicular origin cystic or crateriform features	Lacks sebaceous component Lacks mesenchymal component
Squamous papilloma	Exophytic presentation	Lacks cystic follicular presentation Lacks mesenchymal component Lacks cystic follicular presentation
Sebaceous adenoma	Presence of multiple large lobules of sebaceous cells	Lacks exuberant mesenchymal component Lacks cystic follicular presentation
Sebaceous hyperplasia	Mature sebaceous component	Lacks mesenchymal component Lacks cystic follicular presentation
Basal cell tumor, benign	Dense fibrous stroma may be present	Basal cells predominate Lacks sebaceous epithelial component Lacks cystic follicular presentation
Trichoepithelioma	Follicular origin	Lacks sebaceous epithelial component Formation of rudimentary hair follicles (+/–)
Fibroma	Proliferative fibroblastic component	Lacks sebaceous epithelial component Lacks cystic follicular presentation
Sebaceous trichofolliculoma	Cystic follicular presentation Sebaceous component	Depressed lesion with surface opening Lacks exuberant mesenchymal component typically well-demarcated Collagenous stroma of low cellularity Hair shafts have cystic follicular lumen rudimentary hair follicles (+/–)
Pilomatricoma	Follicular origin	''Ghost'' cells Lacks mesenchymal component Lacks sebaceous epithelial component
Tricholemmoma	Follicular origin	Lacks mesenchymal component Lacks sebaceous epithelial component

''plaque,'' given its association with atherosclerosis in humans, and the possibility of evoking a gross lesion in the minds of some individuals unfamiliar with the nuances of pathology terminology. The audience participants who made these comments expressed the possibility that the term ''plaque'' could be thought to have clinical implications and thus cause problems in interpretation by clinicians and regulators. One participant indicated that the term ''intramural'' implied that the lesion was within the tunica media, and suggested that the term ''subendothelial'' would be better. Several people wished to know how the committee ruled out the possibility that the lesion was an organizing thrombus, with one participant suggesting that serial sections of the lesion could identify neovascularization in the matrix. One participant said that the lesion

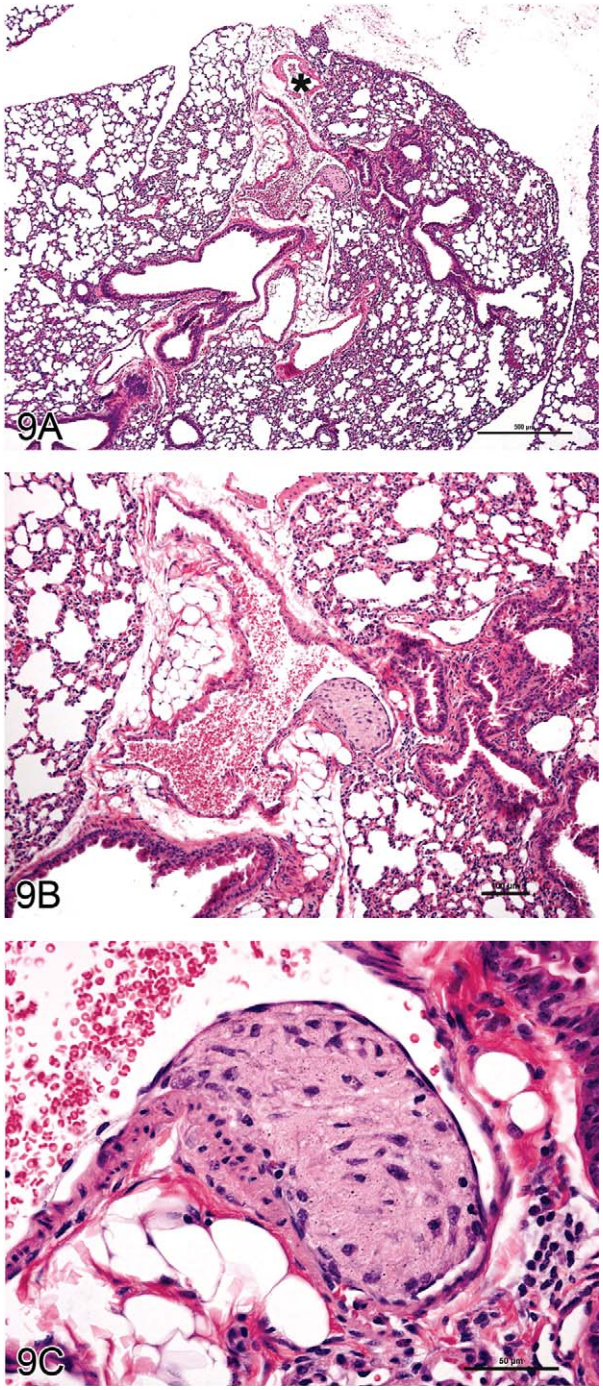

FIGURE 9.—"Intramural plaque" in a blood vessel of the mouse lung. (A–C) Lesion from an untreated manganese superoxide dismutase (MnSOD) mouse. Granular, amorphous material with a spindloid cell component is present between the endothelium and the tunica media; a small focus of similar material is present between the tunica media and the tunica adventitia. The asterisk in (A) indicates a pulmonary vein, identifiable by the cardiomyocytes in the vessel wall. H&E.

occurred at a bifurcation and therefore was not likely to be a thrombus, and another pointed out that it might be an intimal cushion because of its location at a bifurcation. A participant who works with cardiovascular medical devices indicated that if the tissue were "stretched out," the lesion might not be as large as it appears histologically. Another issue raised during the discussion was the question of "When does a thrombus stop being a thrombus?" Thrombi progress from new to organizing to resolving and, at some point, are no longer recognizable as such.

During the discussion, Dr. Wells indicated that the term "plaque" was chosen for the diagnosis in deference to the literature that has been published on the lesion, and that the term "intramural" was selected because the lesion is within the vessel wall. She reiterated that part of the lesion appeared between the tunica media and the adventitia, which is not a typical location for a thrombus. She indicated that the INHAND working group would revisit the proposed term for this lesion based on the comments made during the Satellite Symposium discussion. The subsequent, spirited discussion among the INHAND members was followed by a vote that resulted in retention of "intramural plaque" as the term for this finding. Further discussion will be possible once all proposed INHAND cardiovascular definitions are placed before the global toxicologic pathology community for public comment.

COMPOUND-RELATED SKIN LESIONS IN MICE

Dr. Abraham Nyska (Sackler School of Medicine, Tel Aviv University, Israel), in collaboration with Dr. Yuval Ramot, presented skin lesions in a B6C3F1 mouse from a NTP chronic bioassay in which 3,3',4,4'-tetrachloroazobenzene (TCAB) had been given by gavage. Representative photomicrographs of histologic sections from control (Figure 10A) and treated (Figure 10B) mice were presented with the following diagnostic choices: (1) dermal sclerosis, (2) follicular dilatation and sebaceous gland atrophy, (3) follicular dilatation, (4) hypotrichosis, and (5) another diagnosis. The correct response (determined by peer review), follicular dilatation and sebaceous gland atrophy, was the option favored by the audience (63%). The morphological changes are consistent with chloracne-like lesions.

Chloracne is one of the most common occupational dermatoses and is caused by systemic poisoning with dioxin and dioxin-like compounds (DLCs) (Ramot et al. 2009). It is thought to be mediated by the binding of these compounds to the aryl hydrocarbon receptor, leading to up-regulation of multiple genes involved in xenobiotic metabolism. The exact mechanism by which the skin lesions characteristic of chloracne develop is still obscure. In humans, chloracne is characterized histologically by an acne-like eruption of comedones. Advanced chloracne is typified by non-inflammatory infundibular cysts accompanied by sebaceous gland atrophy. The absence of inflammatory cells is another prominent feature of chloracne (Coenraads et al. 1994; Panteleyev and Bickers 2006; Yamamoto and Tokura 2003). In humans, a striking difference exists in the susceptibility of different hair follicle types to chloracne. While vellus hairs are the most sensitive, scalp follicles are resistant (Panteleyev and Bickers 2006).

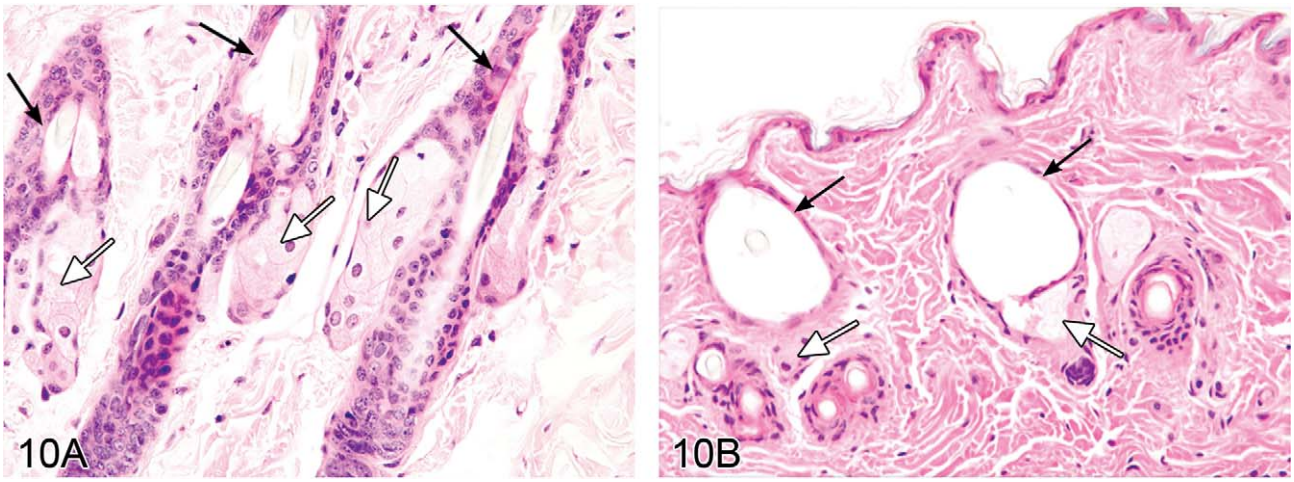

FIGURE 10.—Chloracne in the mouse. (A) Skin from a control male B6C3F1 mouse in the 2-year NTP study for 3,3',4,4'-tetrachloroazobenzene (TCAB). Hair follicles are normal, and adjacent sebaceous glands can be seen. Black arrows indicate hair follicles; open arrows indicate sebaceous glands. (B) Skin from a male B6C3F1 mouse treated for 2 years with TCAB (30 mg/kg). Note dilation of hair follicles, flattening of the epithelial lining, and atrophy of adjacent sebaceous glands. No infiltration of inflammatory cells can be discerned. This animal was assigned a moderate degree of hair follicle dilation (i.e., six or more follicles segmentally dilated to greater than double the normal diameter within a low-magnification field). Black arrows indicate dilated hair follicles; open arrows indicate atrophic sebaceous glands. (Reprinted from Ramot et al. [2009], with permission from Elsevier.) H&E.

In animals, Hill and colleagues (1981) have suggested a classification to evaluate the severity of chloracne lesions according to severity of hair follicle dilatation, the degree of proliferation of the epithelium surrounding the hair follicle or lining the epidermis, and the amount of sebaceous gland atrophy. The Hill criteria were used to study chloracne-like lesions in a series of NTP chronic toxicity and carcinogenicity bioassays in Sprague-Dawley rats that evaluated the effects of dioxin and DLCs (NTP 2006a, 2006b, 2006c, 2006d). One study in particular was performed on mice (B6C3F1), evaluating the toxicity of TCAB (NTP 2009). This study was of special interest because mice, in contrast to rats, are susceptible to dioxin-induced chloracne. Furthermore, a prior study with a structural analog to TCAB, tetrachloroazoxybenzene, revealed chloracne-like lesions in mice after 13 weeks of treatment (Van Birgelen et al. 1999).

Although the incidences of follicular dilatation were significantly increased in both males and females exposed to 10 and 30 mg/kg/day TCAB, and the incidences of sebaceous gland atrophy were significantly increased in males exposed to 10 and 30 mg/kg/day TCAB and in females exposed to 30 mg/kg/day TCAB, severity scores did not differ across dose groups for either evaluated parameter (NTP 2009). In addition, no statistical correlation was found between the presence of follicular dilation and the presence of sebaceous gland atrophy. In contrast to the Hill classification, this study did not show hyperproliferation but, rather, thinning of the epithelium. This is in agreement with the timeline of chloracne lesion formation, which starts with hyperproliferation of keratinocytes and progresses to thinning of the epidermis (Hambrick 1957).

The morphological changes seen in chloracne are suggested to occur from a chloracnegen-induced accelerated exit of cells from the stem cell compartment, which is coupled with a shift towards a keratinized squamous phenotype (Panteleyev and Bickers 2006). Another possible mechanism for the action of dioxin and DLCs may be an indirect effect due to the disruption of retinoid homeostasis in the liver, resulting in abnormal epithelial differentiation to a keratinized squamous phenotype (Schmidt et al. 2003). The ability of dioxin and related compounds to cause altered differentiation of epithelial tissue leading to the squamous phenotype was evident in different organs in the 2-year NTP bioassays. 2,3,7,8-Tetrachlorodibenzo-*p*-dioxin (TCDD), 3,3',4,4',5-pentachlorobiphenyl (PCB 126), 2,3,4,7,8-pentachlorodibenzofuran (PeCDF), and the toxic equivalency factor mixture induced gingival squamous cell hyperplasia and/or squamous cell carcinoma (SCC), endometrial squamous metaplasia and/or SCC, squamous hyperplasia in the forestomach, and squamous metaplasia and/or cystic keratinizing epithelioma and SCC in the lung (NTP 2006a, 2006b, 2006c, 2006d; Walker et al. 2007; Yoshizawa et al. 2005). All these data suggest that a common mechanism might affect selected epithelial tissues, including the skin, and result in alteration of differentiation leading to a squamous type.

Interestingly, in animals the chloracnegenic effects of dioxins and DLCs have been found only in rhino mice, hairless mice, rabbits, and monkeys; while rats, haired mice, and guinea pigs were considered resistant to these effects (Ramot et al. 2009). Until now, no good explanation for these interspecies differences has been found (Panteleyev and Bickers 2006). However, in the current study, we show that one haired mouse strain, B6C3F1, is susceptible to the chloracnegenic effect of DLCs, at least after long exposure to TCAB. It should be noted that in the current study, no clinical or macroscopic hair loss was noted, and the lack of any gross findings may explain the reason why chloracne is only rarely reported in haired animals.

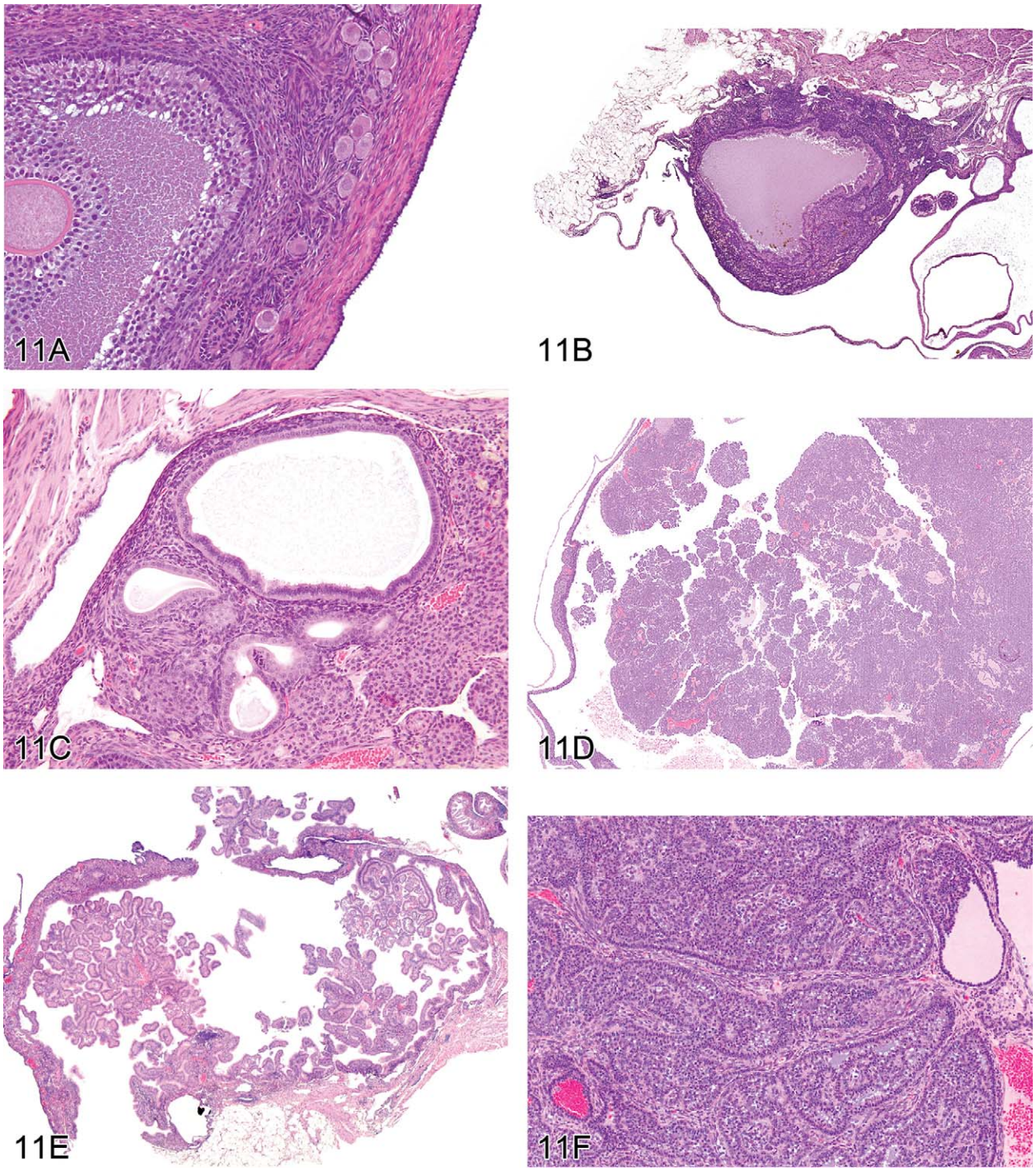

FIGURE 11.—Ovarian proliferative lesions in mice. (A) Normal ovary showing germ cell, stromal, and epithelial elements. (B) Cyst with epithelial hyperplasia. (C) Cystadenoma with adjacent epithelial proliferation. (D) Cystadenocarcinoma. (E) Cystadenoma. (F) Granulosa cell tumor.

MOUSE OVARIAN TUMORS

For the next presentation, Dr. Andrew Suttie (Covance Laboratories, Inc., Vienna, VA, USA) gave a comprehensive overview of mouse ovarian tumors. These neoplasms are derived from one of three compartments of the ovary: epithelium, stroma, or germ cells (Davis, Dixon, and Herbert 1999). The image in Figure 11A illustrates these compartments, and Table 5 provides a list of tumors derived from each compartment.

Epithelial tumors arise from surface epithelium that forms ingrowths into the ovarian stroma. There is a continuum of

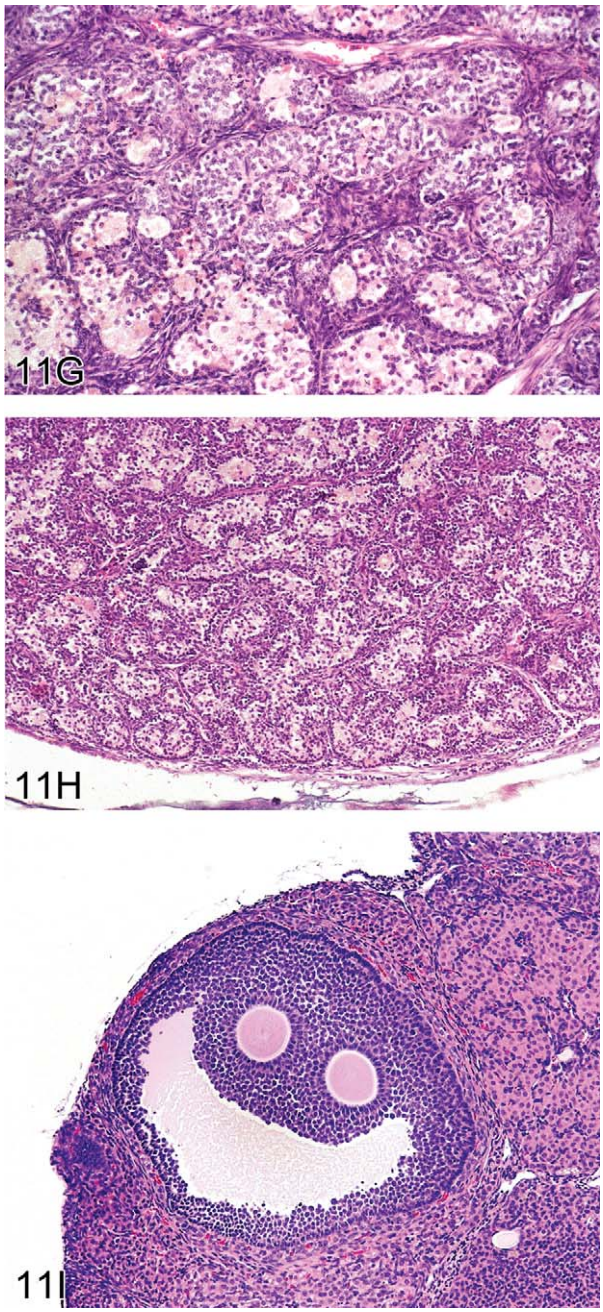

FIGURE 11.—**(continued)** (G) Sertoli cell tumor. (H) Tubulostromal cell tumor. (I) Bi-ovulate follicle from a RasH2 mouse. H&E.

epithelial-derived ovarian lesions. Cysts are dilated cavities, which may be hemorrhagic with hyperplastic epithelium (also referred to as cystic hyperplasia; Figure 11B). Cystadenoma is diagnosed when cystic lesions contain papillary ingrowths, which frequently resemble fallopian tube papillae. The proliferating epithelium can fill and expand the cyst. Lesions may have proliferations of epithelium adjacent to the cyst. The symposium considered one such borderline lesion between hyperplasia and cystadenoma where an epithelial cyst was accompanied by adjacent epithelial proliferation (Figure 11C); a plurality of the participants (44%) agreed that cystadenoma was an appropriate diagnosis. Cystadenocarcinoma (Figure 11D) exhibits multilayered, disorganized epithelium and/or high mitotic or apoptotic indices. In contrast, cystadenoma is the preferred diagnosis for lesions with well-organized papillary ingrowths (Figure 11E). Tubulostromal tumors are also considered to be of epithelial origin in which the ingrowths of epithelium infiltrate the ovarian stroma separating the stromal tissue into packets. As a result of this packeting, these tumors can be difficult to differentiate from some complex stromal tumors.

TABLE 5.—Classification scheme of mouse ovarian tumors.

Germ cell	Dysgerminoma
	Teratoma
	Choriocarcinoma
	Yolk sac carcinoma
Epithelium	Cystadenoma/cystadenocarcinoma
	Tubulostromal adenoma/carcinoma
	Mesothelioma
Sex cord-stromal	Granulosa cell
	Thecoma
	Luteoma
	Sertoli cell
	Stromal cell (including fibroma/fibrosarcoma)

Stromal tumors include granulosa cell, thecal cell, luteal cell, Sertoli cell, and complex stromal tumors. The latter are not differentiated toward any single cell type. Granulosa cell tumors frequently have areas resembling the zona granulosa of the developing follicle (Figure 11F). Thecal cell tumors have more spindle-shaped cells and resemble the theca interna or externa of the follicle. Since the morphology of these two tumors frequently overlaps, they are often combined in the diagnosis of granulosa/thecal cell tumors. Luteomas have cellular morphology similar to the corpus luteum with large eosinophilic cells. Sertoli cell tumors consist of tubular structures resembling Sertoli-only testicular tubules. Complex stromal tumors consist of bundles of cells with varying morphology of multiple stromal cell types and can be difficult to differentiate from tubulostromal cell tumors. The symposium audience considered two examples of lesions with morphology similar to both stromal cell tumors and tubulostromal cell tumors. For Figure 11G, the majority vote was Sertoli cell tumor (38%), while for Figure 11H, the majority vote was tubulostromal tumor (43%).

Dr. Suttie indicated that cysts are very common in carcinogenicity studies with CD1 mice, and therefore consistent diagnostic criteria for differentiating cysts from their neoplastic counterparts is important to reflect accurately potential treatment effects. Stromal tumors occur less frequently, in usually less than 2% of animals. Therefore, maintaining consistent diagnostic criteria between different carcinogenicity studies is important, since reference to historical control data will frequently be necessary to interpret tumor trends in a study. It was commented by an audience member that all stromal tumors should be combined into a single diagnosis when reporting study findings to avoid confusion between different terminologies.

Finally, as a lighthearted aside, the symposium was asked to guess the mouse strain in which the follicle shown in Figure 11I was observed. Although biovulate ovaries are not typical for any mouse strain, the correct answer was RasH2.

ACKNOWLEDGMENTS

The authors wish to thank Eli Ney of the NIEHS for her unique and creative cover artwork for the Symposium handouts as well as for her technical expertise in formatting the speakers' PowerPoint presentations. Thanks are also extended to both Eli Ney and Beth Mahler of EPL for their assistance with image preparation for the article and to David Sabio of EPL for assistance during the Symposium. Appreciation also goes to Sue Pitsch, Krystle Correll, Tierre Miller, and Maureen Kettering of Association Innovation and Management, Inc. (AIM) for their valuable help with annual advertising and meeting facilities. Also integral to the success of this meeting was the security support provided by William Stoeffler and the staff of the Stoeffler Group, LLC.

REFERENCES

Bach, U., Hailey, J. R., Hill, G. D., Kaufmann, W., Latimer, K. S., Malarkey, D. E., Maronpot, R. M., Miller, R. A., Moore, R. R., Morrison, J. P., Nolte, T., Rinke, M., Rittinghausen, S., Suttie, A. W., Travlos, G. S., Vahle, J. L., Willson, G. A., and Elmore, S. A. (2010). Proceedings of the 2009 National Toxicology Program Satellite Symposium. *Toxicol Pathol* **38**, 9–36.

Bannasch, P., and Zerban, H. (1990). Tumours of the liver. In Pathology of Tumours in Laboratory Animals. Vol. I: Tumours of the Rat (V. S. Turusov and U. Mohr, eds.), 2nd ed., pp. 199–240. IARC Scientific Publications No. 99, Lyon, France.

Beaver, D. L. (1960). A re-evaluation of the rat preputial gland as a "dicrine" organ from the standpoint of its morphology, histochemistry, and physiology. *J Exp Zool* **143**, 153–73.

Bennett, G. J., and Xie, Y.-K. (1988). A peripheral mononeuropathy in rat that produces disorders of pain sensation like those seen in man. *Pain* **33,** 87–107.

Best, P. V., and Heath, D. (1961). Interpretation of the appearances of the small pulmonary blood vessels in animals. *Circ Res* **9**, 288–94.

Brigger, D., and Muckle, R. J. (1975). Comparison of Sirius red and Congo red as stains for amyloid in animal tissues. *J Histochem Cytochem* **23**, 84–8.

Coenraads, P. J., Brouwer, A., Olie, K., and Tang, N. (1994). Chloracne. Some recent issues. *Dermatol Clin* **12**, 569–76.

Cooper, J. H. (1969). An evaluation of current methods for the diagnostic histochemistry of amyloid. *J Clin Path* **22**, 410–3.

Davis, B. J., Dixon, D., and Herbert, R. A. (1999). Ovary, oviduct, uterus, cervix and vagina. In Pathology of the Mouse: Reference and Atlas (R. Maronpot, ed.), 1st ed., pp. 409–43. Cache River Press, Vienna, IL.

Deschl, U., Ernst, H., Frantz, J. D., Goodman, D. G., Hartig, F., Konishi, Y., Küttler, K., Popp, J. A., Püschner, H., Squire, R. A., Tatematsu, M., Tuch, K., Ward, J. M., and Whiteley, L. O. (1997). Digestive system. In International Classification of Rodent Tumours Part 1—The Rat (U. Mohr, ed.), pp. 65–98. WHO IARC Scientific Publications No. 122, Lyon, France.

Doi, T., Kokoshima, H., Kanno, T., Sato, J., Wako, Y., Tsuchitani, M., and Matsui, T. (2010). New findings concerning eosinophilic substance deposition in mouse nasal septum: Sex difference and no increase in seniles. *Toxicol Pathol* **38**, 631–6.

Doi, T., Kotani, Y., Kokoshima, H., Kanno, T., Wako, Y., and Tsuchitani, M. (2007). Eosinophilic substance is "not amyloid" in the mouse nasal septum. *Vet Pathol* **44,** 796–802.

Doi, T., Kotani, Y., Kokoshima, H., Kanno, T., Wako, Y., Tsuchitani, M., and Matsui, T. (2009). Deposition process of eosinophilic substance in mouse nasal septum. *J Vet Med Sci* **71**, 931–5.

Ernst, H., Dungworth, D. L., Kamino, K., Rittinghausen, S., and Mohr, U. (1996). Nonneoplastic lesions in the lungs. In Pathobiology of the Aging Mouse (U. Mohr, D. L. Dungworth, C. C. Capen, W. W. Carlton, J. P. Sundberg, and J. M. Ward, eds.), Vol. I, pp. 281–300. ILSI Press, Washington, DC.

Eustis, S. L., Boorman, G. A., Harada, T., and Popp, J. A. (1990). Liver. In Pathology of the Fischer Rat. Reference and Atlas (G. A. Boorman, S. L. Eustis, M. R. Elwell, C. A. Montgomery Jr., and W. F. MacKenzie, eds.), pp. 71–94. Academic Press, San Diego, CA.

Eustis, S. L., Boorman, G. A., and Hyashi, Y. (1990). Exocrine pancreas. In Pathology of the Fischer Rat. Reference and Atlas (G. A. Boorman, S. L. Eustis, M. R. Elwell, C. A. Montgomery Jr., and W. F. MacKenzie, eds.), pp. 95–108. Academic Press, San Diego, CA.

Fraser, H. (1986). Brain tumours in mice with particular reference to astrocytoma. *Food Chem Toxicol* **24**, 105–11.

Frith, C. H., Ward, J. M., and Turusov, V. S. (1994). Tumours of the liver. In Pathology of Tumours in Laboratory Animals. Vol. 2: Tumours of the Mouse (V. S. Turusov and U. Mohr, eds.), 2nd ed., pp. 223–69. IARC Scientific Publications No. 111, Lyon, France.

Giknis, M. L. A., and Clifford, C. B. (2000). *Spontaneous Neoplastic Lesions in the Crl:CD-1 (ICR) BR Mouse*. Charles River Laboratories. http://www.criver.com/sitecollectiondocuments/rm_rm_r_lesions_crl_cd_icr_br_mouse.pdf

Gopinath, C. (1986). Spontaneous brain tumours in Sprague-Dawley rats. *Food Chem Toxic* **24**, 113–20.

Greaves, P. (2007). Liver and pancreas. In Histopathology of Preclinical Toxicity Studies, 3rd ed., pp. 457–514. Elsevier, Amsterdam.

Gross, L. G., Ihrke, P. J., Walder, E. J., and Affolter, V. K. (2005). Follicular tumors. In Skin Diseases of the Dog and Cat, 2nd ed., pp. 605–7. Blackwell, Ames, IA.

Hailey, J. R., Walker, N. J., Sells, D. M., Brix, A. E., Jokinen, M. P., and Nyska, A. (2005). Classification of proliferative hepatocellular lesions in Harlan Sprague-Dawley rats chronically exposed to dioxin-like compounds. *Toxicol Pathol* **33**, 165–74.

Hambrick, G. W., Jr. (1957). The effect of substituted naphthalenes on the pilosebaceous apparatus of rabbit and man. *J Invest Dermatol* **28**, 89–102; discussion, 102–3.

Hebel, R., and Stromberg, M. W. (1976). *Anatomy of the Laboratory Rat*. William & Wilkins, Baltimore, MD.

Herbert, R. A., and Leininger, J. R. (1999). Nose, larynx and trachea. In Pathology of the Mouse (R. R. Maronpot, ed.), 259–92. Cache River Press, Vienna, IL.

Hill, R. H., Jr., Rollen, Z. J., Kimbrough, R. D., Groce, D. F., and Needham, L. L. (1981). Tetrachloroazobenzene in 3,4-dichloroaniline and its herbicidal derivatives: propanil, diuron, linuron, and neburon. *Arch Environ Health* **36**, 11–4.

Hobbs, J. R., and Morgan, A. D. (1963). Fluorescence microscopy with thioflavine-T in the diagnosis of amyloid. *J Pathol Bacteriol* **86**, 437–42.

Kay, J. M. (1992). Blood vessels of the lung. In Treatise on Pulmonary Toxicology. Vol. I: Comparative Biology of the Normal Lung (R. A. Parent, ed.), pp. 163–74. CRC Press, Boca Raton, FL.

Kimbrough, R. D., and Linder, R. E. (1974). Induction of adenofibrosis and hepatomas of the liver in BALB-cJ mice by polychlorinated biphenyls (Aroclor 1254). *J Natl Cancer Inst* **53**, 547–52.

Kimbrough, R. D., Linder, R. E., Burse, V. W., and Jennings, R. W. (1973). Adenofibrosis in the rat liver, with persistence of polychlorinated biphenyls in adipose tissue. *Arch Environ Health* **27**, 390–5.

Kimura, T., Miyazawa, H., Aoyagi, T., and Ackerman, A. B. (1991). Folliculosebaceous cystic hamartoma: A distinctive malformation of the skin. *Am J Dermatopathol* **13**, 213–20.

Klimstra, D. S., Rosai, J., and Heffess, C. S. (1994). Mixed acinar-endocrine carcinomas of the pancreas. *Am J Surg Pathol* **18**, 765–78.

Krinke, G., Naylor, D. C., Schmid, S., Frohlich, E., and Schneider, K. (1985). The incidence of naturally occurring primary brain tumours in the laboratory rat. *J Comp Path* **95**, 175–92.

Langford, L. A., and Barré, G. M. (1997). Tanycytic ependymoma. *Ultrastruct Pathol* **21**, 135–42.

Maekawa, A., Onodera, H., Tanigawa, H., Furuta, K., Takahashi, M., Kurokawa, Y., Kokubo, T., Ogiu, T., Uchida, O., Kobayashi, K., and Hayashi, Y. (1984). Spontaneous tumours of the nervous system and associated organs and/or tissues in rats. *Gann* **75**, 784–91.

Mancini, M. A., Majumdar, D., Chatterjee, B., and Roy, A. K. (1989). $\alpha_{2\mu}$-Globulin in modified sebaceous glands with pheromonal functions: Localization of the protein and its mRNA in preputial, meinbomian, and perinanal glands. *J Histochem Ctyochem* **37**, 149–57.

Marrache, F., Cazals-Hatem, D., Kianmanesh, R., Palazzo, L., Couvelard, A., O'Toole, D., Maire, F., Hammel, P., Levy, P., Sauvanet, A., and Ruszniewski, P. (2005). Endocrine tumor and intraductal papillary mucinous neoplasm of the pancreas: Fortuitous association? *Pancreas* **31**, 79–83.

Mesquita-Guimarães, J., and Coimbra, A. (1974). Acid hydrolases in the perinuclear secretion granules of the rat preputial gland. A light and electron microscope study. *Histochem J* **6**, 685–92.

Mikaelian, I., Ichiki, T., Ward, J. M., and Sundberg, J. P. (2004). Diversity of spontaneous neoplasms in commonly used inbred strains and stocks of laboratory mice. In The Laboratory Mouse (H. J. Hedrich and G. Bullock, eds.), pp. 345–54. Elsevier, London.

Mohr, U. (1994). *International Classification of Rodent Tumors, Part I, The Rat. Fascicle No. 6: Endocrine System*, pp. 56–70, IARC Scientific Publications No. 122, Lyon, France.

National Toxicology Program (NTP) (1989). Toxicology and Carcinogenesis Studies of Nalidixic Acid (CAS No. 389-08-2) in F344/N Rats and B6C3F$_1$ Mice (Feed Studies). NTP Technical Report Series No. 368. NIH Publication No. 90-2823. U.S. Department of Health and Human Services, Public Health Service, National Institutes of Health, Research Triangle Park, NC.

National Toxicology Program (NTP) (1990a). Toxicology and Carcinogenesis Studies of Glycidol (CAS No. 556-52-5) in F344/N Rats and B6C3F$_1$ Mice (Gavage Studies). NTP Technical Report Series No. 374. NIH Publication No. 90-2829. U.S. Department of Health and Human Services, Public Health Service, National Institutes of Health, Research Triangle Park, NC.

National Toxicology Program (NTP) (1990b). Toxicology and Carcinogenesis Studies of 3,3'-dimethoxy-benzidine dihydrochloride (CAS No. 20325-40-0) in F344/N Rats (Drinking Water Studies). NTP Technical Report Series No. 372. NIH Publication No. 90-2827. U.S. Department of Health and Human Services, Public Health Service, National Institutes of Health, Research Triangle Park, NC.

National Toxicology Program (NTP) (1991a). Toxicology and Carcinogenesis Studies of C. I. Acid Red 114 (CAS No. 6459-94-5) in F344/N Rats (Drinking Water Studies). NTP Technical Report Series No. 405. NIH Publication No. 92-3136. U.S. Department of Health and Human Services, Public Health Service, National Institutes of Health, Research Triangle Park, NC.

National Toxicology Program (NTP) (1991b). Toxicology and Carcinogenesis Studies of 3,3'-dimethyl-benzidine dihydrochloride (CAS No. 612-82-8) in F344/N Rats (Drinking Water Studies). NTP Technical Report Series No. 390. NIH Publication No. 91-2845. U.S. Department of Health and Human Services, Public Health Service, National Institutes of Health, Research Triangle Park, NC.

National Toxicology Program (NTP) (1992). Toxicology and Carcinogenesis Studies of C. I. Direct Blue 15 (Desalted Industrial Grade) (CAS No. 2429-74-5) in F344/N Rats (Drinking Water Studies). NTP Technical Report Series No. 397. NIH Publication No. 92-2852. U.S. Department of Health and Human Services, Public Health Service, National Institutes of Health, Research Triangle Park, NC.

National Toxicology Program (NTP) (1993a). Toxicology and Carcinogenesis Studies of 1, 2, 3-trichloropropane (CAS No. 96-18-4) in F344/N Rats and B6C3F$_1$ Mice (Gavage Studies). NTP Technical Report Series No. 384. NIH Publication No. 94-2839. U.S. Department of Health and Human Services, Public Health Service, National Institutes of Health, Research Triangle Park, NC.

National Toxicology Program (NTP) (1993b). Toxicology and Carcinogenesis Studies of 2, 3-dibromo-1-propanol (CAS No. 9613-9) in F344/N Rats and B6C3F$_1$ Mice (Dermal Studies). NTP Technical Report Series No. 400. NIH Publication No. 94-2855. U.S. Department of Health and Human Services, Public Health Service, National Institutes of Health, Research Triangle Park, NC.

National Toxicology Program (NTP) (1996). Toxicology and Carcinogenesis Studies of 1-amino-2,4-dibromoanthraquinone (CAS No. 81-49-2) in F344/N Rats and B6C3F1 Mice (Feed Studies). NTP Technical Report Series No. 383. NIH Publication No. 96-2838. U.S. Department of Health and Human Services, Public Health Service, National Institutes of Health, Research Triangle Park, NC.

National Toxicology Program (NTP) (2000). Toxicology and Carcinogenesis Studies of Methyleugenol (CAS No. 93-15-2) in F344/N Rats and B6C3F1 Mice (Gavage Studies). NTP Technical Report Series No. 491. NIH Publication No. 00-3950. U.S. Department of Health and Human Services, Public Health Service, National Institutes of Health, Research Triangle Park, NC.

National Toxicology Program (NTP) (2006a). Toxicology and Carcinogenesis Studies of a Mixture of 2,3,7,8-tetrachlorodibenzo-*p*-dioxin (TCDD) (CAS No. 1746-01-6), 2,3,4,7,8-pentachlorodibenzofuran (PeCDF) (CAS No. 57117-31-4), and 3,3',4,4',5-pentachlorobiphenyl (PCB126) (CAS No. 57465-28-8) in Female Harlan Sprague-Dawley Rats (Gavage Studies). TR526. U.S. Department of Health and Human Services, Public Health Service, National Institutes of Health, Research Triangle Park, NC.

National Toxicology Program (NTP) (2006b). Toxicology and Carcinogenesis Studies of 3,3',4,4',5-pentachlorobiphenyl (PCB126) (CAS No. 57465-28-8) in Female Harlan Sprague-Dawley Rats (Gavage Studies). TR520. U.S. Department of Health and Human Services, Public Health Service, National Institutes of Health, Research Triangle Park, NC.

National Toxicology Program (NTP) (2006c). Toxicology and Carcinogenesis Studies of 2,3,4,7,8-pentachlorodibenzofuran (PeCDF) (CAS No. 57117-31-4) in Female Harlan Sprague-Dawley Rats (Gavage Studies). TR525. U.S. Department of Health and Human Services, Public Health Service, National Institutes of Health, Research Triangle Park, NC.

National Toxicology Program (NTP) (2006d). Toxicology and Carcinogenesis Studies of 2,3,7,8-tetrachloribenzo-*p*-dioxin (TCDD) (CAS No. 1746-01-6) in Female Harlan Sprague-Dawley Rats (Gavage Studies). TR521. U.S. Department of Health and Human Services, Public Health Service, National Institutes of Health, Research Triangle Park, NC.

National Toxicology Program (NTP) (2009). Toxicology and Carcinogenesis Studies of 3,3',4,4'-tetrachloroazobenzene (TCAB) (CAS No. 14047-09-7) in Harlan Sprague-Dawley Rats and B6C3F1 Mice (Gavage Studies). TR558. U.S. Department of Health and Human Services, Public Health Service, National Institutes of Health, Research Triangle Park, NC.

Newman, K., Stahl-Herz, J., Kabiawu, O., Newman, E., Wieczorek, R., Wang, B., Pei, Z., Bannan, M., Lee, P., and Xu, R. (2009). Pancreatic carcinoma with multilineage (acinar, neuroendocrine, and ductal) differentiation. *Int J Exp Pathol* **2**, 602–7.

Orsulak, P. J., and Gawienowski, A. M. (1972). Olfactory preferences for the rat preputial gland. *Biol Reproduction* **6**, 219–23.

Panteleyev, A. A., and Bickers, D. R. (2006). Dioxin-induced chloracne—reconstructing the cellular and molecular mechanisms of a classic environmental disease. *Exp Dermatol* **15**, 705–30.

Poppleton, H., and Gilbertson, R. J. (2007). Stem cells of ependymoma. *Br J Cancer* **96**, 6–10.

Radovsky, A., and Mahler, J. (1999). The nervous system. In Pathology of the Mouse: Reference and Atlas (R. R. Maronpot, ed.), 1st ed., pp. 445–70. Cache River Press, Vienna, IL.

Ramdial, P. K., Chrystal, V., and Madaree, A. (1998). Folliculosebaceous cystic hamartoma. *Pathology* **30**, 212–4.

Ramot, Y., Nyska, A., Lieuallen, W., Maly, A., Flake, G., Kissling, G. E., Brix, A., Malarkey, D. E., and Hooth, M. J. (2009). Inflammatory and

chloracne-like skin lesions in B6C3F1 mice exposed to 3,3',4,4'-tetrachloroazobenzene for 2 years. *Toxicology* **265**, 1–9.

Ramot, Y., Steiner, M., Morad, V., Leibovitch, S., Amouyal, N., Cesta, M., and Nyska, A. (2010). Pulmonary thrombosis in the mouse following intravenous administration of quantum dot-labeled mesenchymal cells. *Nanotoxicology* **4**, 98–105.

Rehm, S., Wcislo, A., and Deerberg, F. (1985). Non-neoplastic lesions of female virgin Han:NMRI mice, incidence and influence of food restriction throughout life span. II: Respiratory tract. *Lab Anim* **19**, 224–35.

Renne, R., Brix, A., Harkema, J., Herbert, R., Kittel, B., Lewis, D., March, T., Nagano, K., Pino, M., Rittinghausen, S., Rosenbruch, M., Tellier, P., and Wohrmann, T. (2009). Proliferative and nonproliferative lesions of the rat and mouse respiratory tract. *Toxicol Pathol* **37** (Suppl. 7), 5S–73S.

Reznik, G., and Ward, J. M. (1981). Morphology of neoplastic lesions in the clitoral and prepucial gland of the F344 rat. *J Cancer Res Clin Oncol* **101**, 249–63.

Riley, M. G. I., Boorman, G. A., McDonald, M. M., Longnecker, D., Solleveld, H. A., and Giles, H. D. (1990). Proliferative and metaplastic lesions of the endocrine pancreas in rats. In Guides for Toxicologic Pathology. STP/ARP/AFIP, Washington, DC.

Schmidt, C. K., Hoegberg, P., Fletcher, N., Nilsson, C. B., Trossvik, C., Hakansson, H., and Nau, H. (2003). 2,3,7,8-Tetrachlorodibenzo-p-dioxin (TCDD) alters the endogenous metabolism of all-trans-retinoic acid in the rat. *Arch Toxicol* **77**, 371–83.

Schwartz, M. M. (2007). Glomerular diseases with organized deposits. In Heptinstall's Pathology of the Kidney (J. C. Jeannette, J. L. Olson, M. M. Schwartz, and F. G. Silva, eds.), 6th ed., Vol. II, pp. 917–30. Lippincott Williams & Wilkins, Philadelphia, PA.

Senaldi, G., Stolina, M., Guo, J., Faggioni, R., McCabe, S., Kaufman, S. A., Van, G., Xu, W., Fletcher, F.A., Boone, T., Chang, M. S., Sarmiento, U., and Cattley, R. C. (2002). Regulatory effects of novel neurotrophin-1/B cell-stimulating factor-3 (cardiotropin-like cytokine) on B cell function. *J Immunol* **168**(11), 5690–5698.

Sirica, A. E. (1992). *The Role of Cell Types in Hepatocarcinogenesis*. CRC Press, Boca Raton, FL.

Takahashi, M., Kawaguchi, M., Shimada, K., Konishi, N., Furuya, H., and Nakashima, T. (2004). Cyclooxygenase-2 expression in Schwann cells and macrophages in the sciatic nerve after single spinal nerve injury in rats. *Neurosci Lett* **363,** 203–6.

Taylor, M. D., Poppleton, H., Fuller, C., Su, X., Liu, Y., Jensen, P., Magdaleno, S., Dalton, J., Calabrese, C., Board, J., MacDonald, T., Rutka, J., Guha, A., Gajjar, A., Curran, T., and Gilbertson, R. J. (2005). Radial glial cells are candidate stem cells of ependymoma. *Cancer Cell* **8**, 323–35.

Terada, T., Matsunaga, Y., Maeta, H., Endo, K., Horie, S., and Ohta, T. (1999). Mixed ductal-endocrine carcinoma of the pancreas presenting as gastrinoma with Zollinger-Ellison syndrome: An autopsy case with a 24-year survival period. *Virchows Arch* **435**, 606–11.

Van Birgelen, A. P., Hebert, C. D., Wenk, M. L., Grimes, L. K., Chapin, R. E., Travlos, G. S., Mahler, J., and Bucher, J. (1999). Toxicity of 3,3',4,4'-tetrachloroazoxybenzene in rats and mice. *Toxicol Appl Pharmacol* **156**, 206–21.

Walker, N., Yoshizawa, K., Miller, R. A., Brix, A. E., Sells, D. M., Jokinen, M. P., Wyde, M. E., Easterling, M., and Nyska, A. (2007). Pulmonary lesions in female Harlan Sprague-Dawley rats following two-year oral treatment with dioxin-like compounds. *Tox Pathol* **35**, 880–9.

Ward, J. M., and Rice, J. M. (1982). Naturally occurring and chemically induced brain tumours of rats and mice in carcinogenesis bioassays. *Ann NY Acad Sci* **381**, 304–19.

Wojcinski, Z. W., Albassam, M. A., and Smith, G. S. (1991). Hyaline Glomerulopathy in B6C3F1 Mice. *Toxicol Pathol* **19**, 224–229.

Yamamoto, O., and Tokura, Y. (2003). Photocontact dermatitis and chloracne: two major occupational and environmental skin diseases induced by different actions of halogenated chemicals. *J Dermatol Sci* **32**, 85–94.

Yamate, J., Tajima, M., Nunoya, T., and Kudow, S. (1987). Spontaneous tumours of the central nervous system of Fischer 344/Du Crj rats. *Jpn J Vet Sci* **49,** 67–75.

Yanoff, K., Zimmerman, L. E., and Davis, R. L. (1971). Massive gliosis of the retina. *Int Ophthalmol Clin* **11**, 211–29.

Yoshitomi, K., and Boorman, G. A. (1990). Eye and associated glands. In Pathology of the Fischer Rat. Reference and Atlas (G. A. Boorman, S. L. Eustis, M. R. Elwell, C. A. Montgomery Jr., and W. F. MacKenzie, eds.), pp. 239–338. Academic Press, San Diego, CA.

Yoshizawa, K., Walker, N. J., Jokinen, M. P., Brix, A. E., Sells, D. M., Marsh, T., Wyde, M. E., Orzech, D., Haseman, J. K., and Nyska, A. (2005). Gingival carcinogenicity in female Harlan Sprague-Dawley rats following two-year oral treatment with 2,3,7,8-tetrachlorodibenzo-*p*-dioxin and dioxin-like compounds. *Toxicol Sci* **83**, 64–77.